Bioorganic & Medicinal Chemistry 21 (2013) 2856–2867

Contents lists available at SciVerse ScienceDirect

Bioorganic & Medicinal Chemistry

journal homepage: www.elsevier.com/locate/bmc

Discovery of 3-phenyl-1*H*-5-pyrazolylamine derivatives containing a urea pharmacophore as potent and efficacious inhibitors of FMS-like tyrosine kinase-3 (FLT3)

Wen-Hsing Lin [†], John T.-A. Hsu [†], Shu-Yi Hsieh [†], Chiung-Tong Chen, Jen-Shin Song, Shih-Chieh Yen, Tsu Hsu, Cheng-Tai Lu, Chun-Hwa Chen, Ling-Hui Chou, Yung-Ning Yang, Ching-Hui Chiu, Ching-Ping Chen, Ya-Ju Tseng, Kuei-Jung Yen, Ching-Fang Yeh, Yu-Sheng Chao, Teng-Kuang Yeh *, Weir-Torn Jiaang *

Institute of Biotechnology and Pharmaceutical Research, National Health Research Institutes, No. 35, Keyan Rd., Zhunan Town, Miaoli Country 350, Taiwan, ROC

ARTICLE INFO

Article history:
Received 4 February 2013
Revised 28 March 2013
Accepted 30 March 2013
Available online 6 April 2013

Keywords:
FMS-like tyrosine kinase-3
Inhibitor
Acute myeloid leukemia
Receptor tyrosine kinase
Internal tandem duplications

ABSTRACT

Preclinical investigations and early clinical trials suggest that FLT3 inhibitors are a viable therapy for acute myeloid leukemia. However, early clinical data have been underwhelming due to incomplete inhibition of FLT3. We have developed 3-phenyl-1*H*-5-pyrazolylamine as an efficient template for kinase inhibitors. Structure–activity relationships led to the discovery of sulfonamide, carbamate and urea series of FLT3 inhibitors. Previous studies showed that the sulfonamide **4** and carbamate **5** series were potent and selective FLT3 inhibitors with good in vivo efficacy. Herein, we describe the urea series, which we found to be potent inhibitors of FLT3 and VEGFR2. Some inhibited growth of FLT3-mutated MOLM-13 cells more strongly than the FLT3 inhibitors sorafenib (**2**) and ABT-869 (**3**). In preliminary in vivo toxicity studies of the four most active compounds, **10f** was found to be the least toxic. A further in vivo efficacy study demonstrated that **10f** achieved complete tumor regression in a higher proportion of MOLM-13 xenograft mice than **4** and **5** (70% vs 10% and 40%). These results show that compound **10f** possesses improved pharmacologic and selectivity profiles and could be more effective than previously disclosed FLT3 inhibitors in the treatment of acute myeloid leukemia.

1. Introduction

The FMS-like tyrosine kinase-3 (FLT3) is a member of the class III membrane-bound receptor tyrosine kinase (RTK) family, together with cKIT, FMS, and PDGFR.[1,2] Inhibition of RTK signaling pathways has become an important area of new cancer drug discovery,[3–5] particularly for the treatment of acute myeloid leukemia (AML), the most common type of leukemia in adults. AML is an aggressive disease with rapid growth of abnormal leukemic cells in bone marrow that inhibits production of normal blood cells. Despite the success of conventional chemotherapy, the rate of relapse amongst AML patients is relatively high. The failure of initial chemotherapy and the refractory nature of AML have been associated with mutations that activate signal transduction pathways, resulting in enhanced proliferation and survival of leukemia cells.[6,7] Activating mutations in FLT3 are present in ~30% of AML patients.[2,8] These mutations are generally internal tandem duplications (ITDs) in the juxtamembrane domain of the receptor and the missense point, or short-length mutations in the activation loop of the tyrosine kinase domain (TKD).[9–11] In addition to mutant forms of FLT3, wt-FLT3 is highly expressed in most cases of acute leukemia, and FLT3 over-expression is an unfavorable prognostic factor for overall survival in AML. Also, over-expressed wt-FLT3 has the same sensitivity to FLT3 inhibitors as the FLT3/ITD mutants.[12,13]

Due to the prevalence and refractory nature of FLT3 mutations, as well as the poor prognosis for those affected by it, numerous agents have been developed to directly inhibit wild-type and mutant FLT3. Several of these, such as AC220 (**1**),[14] sorafenib (BAY-43-9006, **2**)[15] and ABT-869 (**3**)[16] (Fig. 1), have been investigated as potential agents for the treatment of AML.[17] However, early clinical data for direct FLT3 inhibitors has been underwhelming, with a limited reduction in bone marrow blasts and weak short-term responses. It has been suggested that this is mainly due to low potency and/or inadequate toleration of the inhibitors at effective doses, which together result in a failure to achieve complete and sustained inhibition of FLT3 in patients' leukemic blast cells. Second-generation FLT3 inhibitors which are highly

* Corresponding authors. Tel.: +886 37 246166x35712; fax: +886 37 586456 (W.-T.J.).
E-mail address: wtjiaang@nhri.org.tw (W.-T. Jiaang).
† These authors contributed equally to this work.

0968-0896/$ - see front matter © 2013 Published by Elsevier Ltd.
http://dx.doi.org/10.1016/j.bmc.2013.03.083

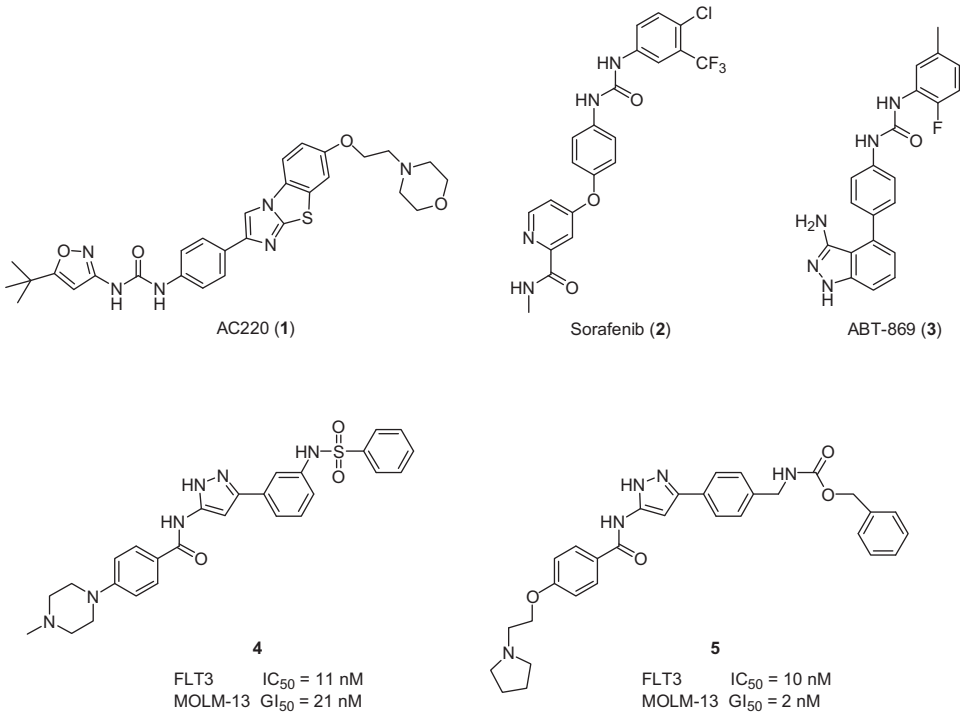

Figure 1. Previously reported FLT3 inhibitors.

potent against both wt-FLT3 and mutants, highly selective, and less toxic than their predecessors, are therefore urgently required.[14,17,18]

Using structure-based design, we previously developed a novel class of 3-phenyl-1*H*-5-pyrazolylamine derivatives (Fig. 2), a versatile template for the development of specific kinase inhibitors, and successfully identified a sulfonamide-substituted series of benzamides (Structure **I**) inhibiting both FLT3 and cellular proliferation.[19] Using rational design, we identified a second sulfonamide-substituted series of pyrimidines (Structure **L**)[19,20] and two carbamate-substituted series of benzamides and pyrimidines (Structures **J** and **M**, respectively)[21] as potent inhibitors of FLT3 (Fig. 2). Representative sulfonamide (**4**) and carbamate (**5**) FLT3 inhibitors are shown in Figure 1. Continuing our efforts to develop potent FLT3 inhibitors, we searched for another series of 3-phenyl-1*H*-5-pyrazolylamine-based inhibitors capable of greater inhibition of AML MOLM-13 cell growth in vitro and with a prolonged duration of action in vivo. In this study, the structure–activity relationships (SAR) and in vitro properties of two urea-substituted series of benzamides (Structure **K**) and pyrimidines (Structure **N**) are reported. Western blots illustrating **10f**'s mechanism of action are also presented. This study led to the discovery of urea **10f** with greater in vivo efficacy than sulfonamide **4** and carbamate **5**.

2. Chemistry

The general synthetic route to the 3-phenyl-1*H*-5-pyrazolylamine benzamides **9** and **10** (Table 1) is depicted in Scheme 1. The synthesis began with 4-nitro or 4-CH_2NHCbz substituted 3-phenyl-1*H*-5-pyrazolylamine **6**, prepared according to literature procedures.[22,23] Benzoyl chlorides **7** with water-solubilizing substituents were prepared from the corresponding acids, which were either commercially available or prepared according to modified

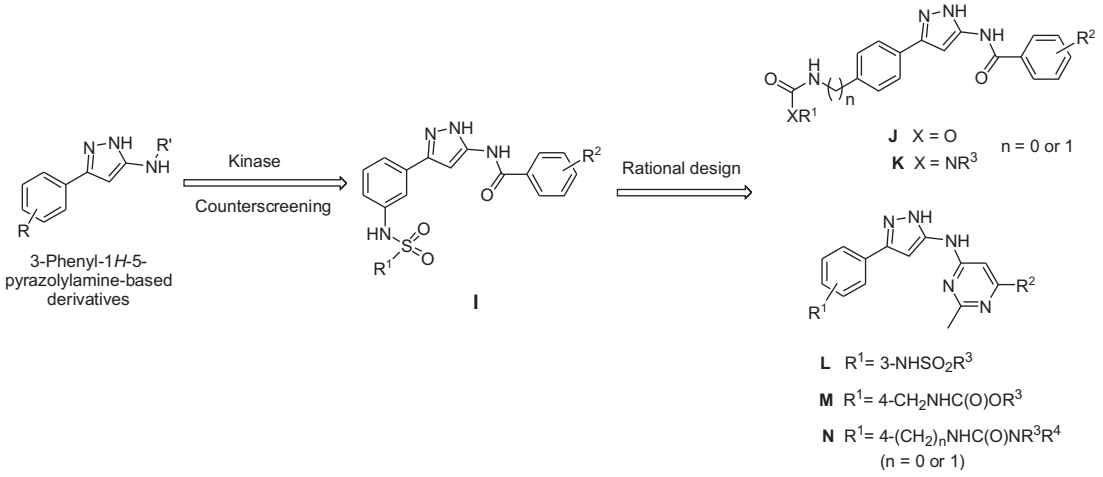

Figure 2. Identification of 3-phenyl-1*H*-5-pyrazolylamine derivatives as FLT3 inhibitors.

Table 1
Inhibition of enzymes and cell proliferation by urea analogues **K**

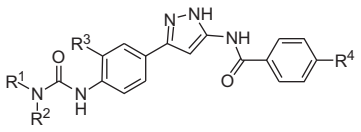

9

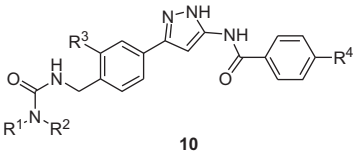

10

Compd	R^1, R^2	R^3	R^4	IC_{50}[a] (μM)			GI_{50}[a] (μM)
				wt-FLT3	VEGFR2	Aurora A	MOLM-13 cell
4				0.011	0.13	0.34	0.021
5				0.010	0.12	>1.0	0.002
9a	C_6H_5, H	H	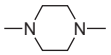	0.013	0.026	0.33	0.006
9b	C_2H_5, H	H	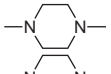	0.094	0.10	>1.0	0.033
9c	C_3H_5, H	H	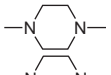	0.052	0.30	>1.0	0.018
9d		H	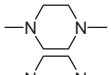	0.070	>1.0	>1.0	0.037
9e	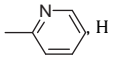	H	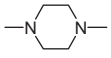	0.040	0.073	0.61	0.042
9f	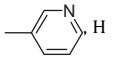	H	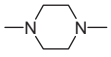	0.074	0.19	0.30	0.022
9g	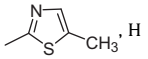	H	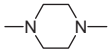	0.050	0.035	0.065	0.009
9h	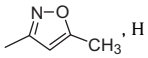	H		0.006	0.031	0.12	0.003
9i	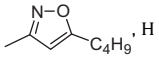	H	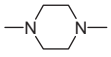	0.030	0.012	0.053	0.005
9j	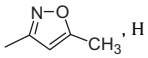	CH_3	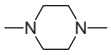	0.009	0.038	0.25	0.001
9k	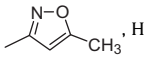	Cl	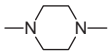	0.39	>1.0	0.60	0.007
9l	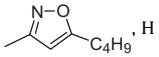	H	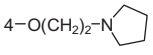	0.015	0.012	0.047	0.002
9m	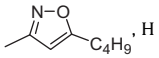	H	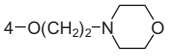	0.019	0.022	0.16	0.002
9n	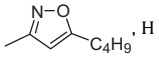	H	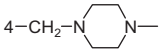	0.008	0.012	0.16	0.001
9o	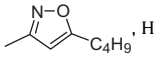	CH_3	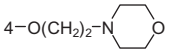	0.020	0.027	0.069	0.008
9p	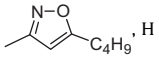	CH_3	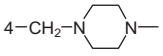	0.002	0.007	0.073	0.002
10a	C_6H_5, H	H	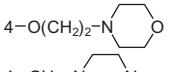	0.009	0.054	0.76	0.003
10b	C_6H_5, H	H	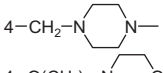	0.022	0.082	>1.0	0.004
10c	4-F-C_6H_5, H	H	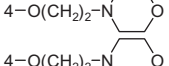	0.066	0.13	>1.0	0.005
10d	4-Cl-C_6H_5, H	H	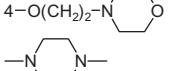	0.016	0.071	>1.0	0.003
10e	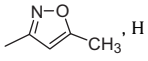	H	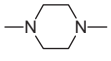	0.013	0.050	0.94	0.002
10f	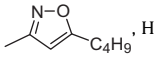	H	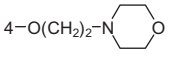	0.018	0.028	>1.0	0.003
10g	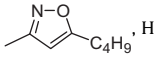	H		0.004	0.018	>1.0	0.003

[a] IC_{50} and GI_{50} values are the means of at least two independent experiments.

literature procedures.[24] These substituted benzoyl chlorides **7** were employed to acylate amines **6** in pyridine to give amides. Reduction of the nitro or Cbz groups using a Pd/C catalyst under H_2 yielded the corresponding amines **8**. These were coupled with alkyl or benzyl isocyanates, or heteroaryl carbamic acid 4-nitrophenyl esters, to afford the corresponding ureas **9** or **10**.

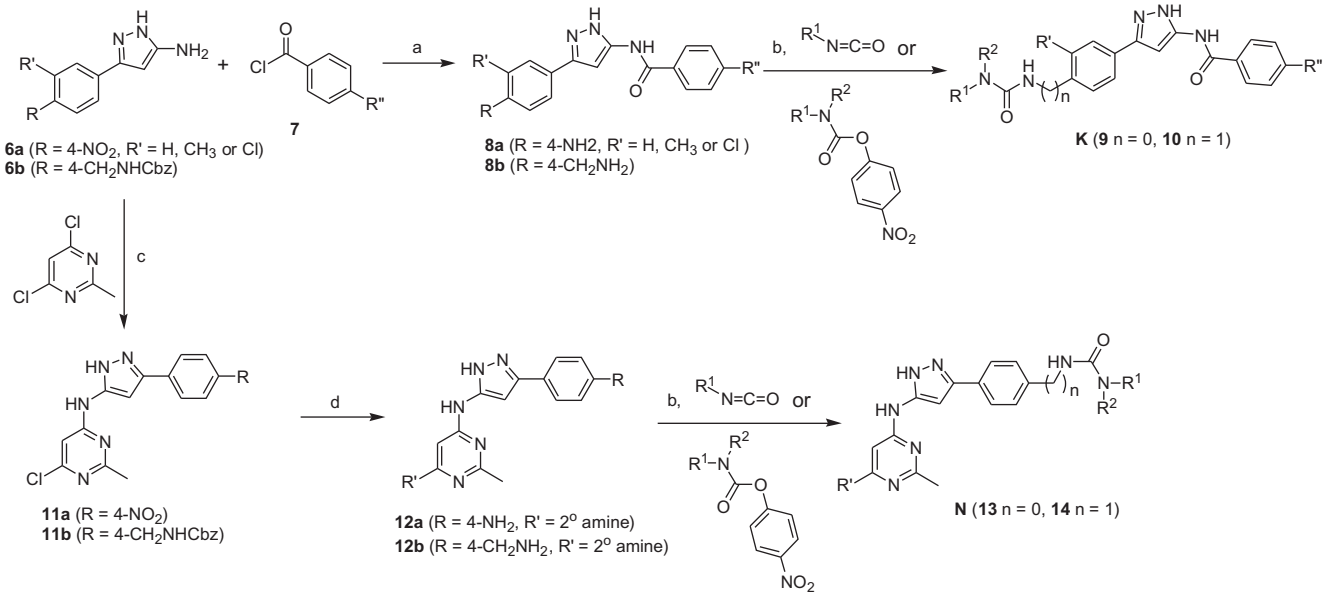

Scheme 1. Reagents and conditions: (a) (i) pyridine, rt, (ii) H_2, Pd/C, MeOH/HCl (aq); (b) pyridine, rt or DMSO, $NaHCO_3$, 50 °C; (c) 4 N HCl/1,4-dioxane, DMF, 80 °C; (d) (i) 2° amines, pyridine, 80 °C, (ii) H_2, Pd/C, MeOH/HCl (aq).

The general synthetic route to the 3-phenyl-1*H*-5-pyrazolyl-amine pyrimidines **13**–**14** (Table 2) is shown in Scheme 1. Treatment of 3-phenyl-1*H*-5-pyrazolylamine **6** with 4,6-dichloropyrimidine, in the presence of 4 N HCl in 1,4-dioxane and DMF at 80 °C, provided 4-monosubstituted pyrimidine derivatives **11**. Treatment of these derivatives with substituted or unsubstituted piperazine in pyridine at 80 °C gave 4,6-disubstituted pyrimidines, which were reduced with Pd/C under H_2 to yield the corresponding amines **12**. These were coupled with alkyl or benzyl-substituted isocyanates, or heteroaryl carbamic acid 4-nitro-phenyl esters to obtain the final pyrimidine ureas **13** or**14**.

3. Biological evaluation

3.1. In vitro pharmacology

As shown in Table 1, the target compounds were tested against FLT3, vascular endothelial growth factor receptor 2 (VEGFR2), and

Table 2
Inhibition of enzymes and cell proliferation by urea analogues **N**

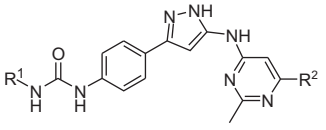

13

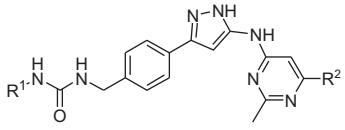

14

Compd	R^1	R^2	IC_{50}[a] (μM)			GI_{50}[a] (μM)
			wt-FLT3	VEGFR2	Aurora A	MOLM-13 cell
13	C_6H_5	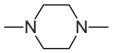	0.28	0.62	0.50	0.16
14a	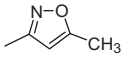	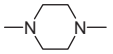	0.021	0.10	0.32	0.009
14b	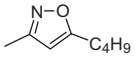	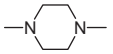	0.035	0.012	0.12	0.003
14c	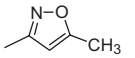	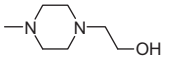	0.017	0.12	0.098	0.016
14d	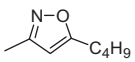	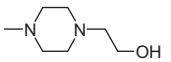	0.095	0.05	0.49	0.005
14e	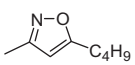	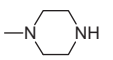	0.026	0.085	0.71	0.008
14f	3-Cl-C_6H_5	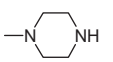	0.026	0.038	0.79	0.018
1			0.069	0.43	>10	0.004
2			0.054	0.020	3.8	0.056
3			0.020	0.007	0.76	0.037

[a] IC_{50} and GI_{50} values are the means of at least two independent experiments.

aurora A kinase (in-house kinas assays), and further evaluated against the mutant FLT3 AML cell line MOLM-13. Previous studies showed that sulfonamides **4** and carbamates **5** were potent and selective FLT3 inhibitors (FLT3 IC_{50} = 0.01 μM; VEGFR2 and aurora A IC_{50} >0.1 μM, Table 1). An extensive SAR study was firstly carried out, replacing the carbamate moiety of **J** (n = 0, Fig. 2) with a urea moiety to give potential **K**-based FLT3 inhibitors. These have a urea group at the 4-position of the phenyl ring, connected to pyrazolylamine at the 3-position (phenylurea compounds **9a**–**p**). The first compound **9a**, with a phenyl substituent at R^1 and a 4-methylpiperazine at R^4, was found to potently inhibit FLT3 (IC_{50} = 0.013 μM) and VEGFR2 (IC_{50} = 0.026 μM). Compound **9a** also weakly inhibited aurora A (IC_{50} = 0.33 μM) and potently inhibited growth of MOLM-13 cells (GI_{50} = 0.006 μM). A significant drop in potency was observed in all assays when the terminal phenyl ring of the urea was replaced by alkyl groups such as ethyl (**9b**), cyclopropyl (**9c**), or amine NR^1R^2, together yielding a five-membered monocyclic ring (**9d**).

Compound **9a**, bearing a phenyl substituent at R^1, is a potent FLT3 inhibitor; however, it is poorly soluble in organic solvents. To overcome this problem, the R^1 substituent of **9a** was changed from a phenyl group to heteroaryl groups. As expected, compounds **9e**–**p** were more soluble in organic solvents, and easily purified by flash column chromatography. In comparison with **9a**, pyridin-2-yl (**9e**) and pyridin-3-yl rings (**9f)** decreased inhibitory activity against wt-FLT3 and VEGFR2, and also against MOLM-13 cells. With a five-membered heteroaryl ring, thiazol-2-yl compound **9g** was 4 times less potent against FLT3 (IC_{50} = 0.05 μM), but maintained potency against MOLM-13 cells (IC_{50} = 0.009 μM) relative to phenyl compound **9a**. 5-Methyl-isoxazole **9h** and 5-*tert*-butyl-isoxazole **9i** potently inhibited growth of MOLM-13 cells (GI_{50} = 0.003 and 0.005 μM, respectively); but 5-*tert*-butyl-isoxazole **9i** was only half as potent as **9a** in FLT3 inhibition. Five-membered heteroaryl compounds **9g**–**i** were potent VEGFR2 inhibitors (IC_{50} = 0.012–0.035 μM), and potent to moderate inhibitors of aurora A (IC_{50} = 0.053–0.12 μM).

Next, we examined the effects of the R^3 substituent on the phenyl ring connected to the pyrazolylamine group at the 3-position. Compound **9j**, with a methyl substituent at R^3, potently inhibited FLT3 and VEGFR2 (IC_{50} = 0.009 and 0.038 μM, respectively), and very potently inhibited growth of MOLM-13 cells (GI_{50} = 0.001 μM). Chlorination at R^3 (**9k**) dramatically decreased potency against FLT3 and VEGFR2 (FLT3 IC_{50} = 0.39 μM, VEGFR2 IC_{50} >1.0 μM). Nevertheless, **9k** still exhibited a GI_{50} value of 0.007 μM against MOLM-13 cells.

Previous studies have demonstrated the importance of a water-solubilizing substituent on the benzamide for optimal activity.[20,21] The SAR of ureas with various water-solubilizing benzamide substituents (R^4) was similar to that displayed in the carbamate series.[21] Conserving the 5-*tert*-butyl-isoxazole urea moiety, a pyrrolidine (**9l**) or morpholine group (**9m**) tethered by a two-carbon ether or a *N*-methylpiperazine group (**9n**) linked by a one-carbon tether potently inhibited FLT3 and VEGFR2, comparable in potency to *N*-methylpiperazine **9i** in both cases (FLT3 IC_{50} = 0.008–0.019 μM, VEGFR2 IC_{50} = 0.012–0.022 μM). Compounds **9l**–**n** were more potent against MOLM-13 cells (GI_{50} = 0.001–0.002 μM) than the *N*-methylpiperazine analogue **9i** (GI_{50} = 0.005 μM). 5-*tert*-Butyl-isoxazole ureas **9i** and **9l**–**n** bearing different water-solubilizing substituents displayed moderate to potent inhibition of aurora A (IC_{50} = 0.047–0.16 μM). When R^3 was substituted with a methyl group, the resulting compound **9o** showed a fourfold lost of potency compared to the unsubstituted analogue **9m** (R^3 = H). Compound **9p** bearing an *N*-methylpiperazine group was the most potent FLT3 inhibitor (IC_{50} = 0.002 μM) in this series. It had a GI_{50} value of 0.002 μM against MOLM-13 cells and was fourfold more potent than the R^3 unsubstituted analogue **9n** in FLT3 enzyme-inhibition assay. Compounds **9o** and **9p** both exhibited potent inhibition against VEGFR2 (IC_{50} <30 nM) and aurora A (IC_{50}—70 nM) kinases.

Having demonstrated the importance of the urea pharmacophore, SAR studies to investigate the effect of chain length between the urea moiety and the 4-position of the phenyl ring were carried out (benzylurea compounds **10a**–**g**, Table 1). When R^1 was a phenyl group, compounds **10a** and **10b** (possessing different water-solubilizing substituents) inhibited FLT3 and MOLM-13 cell growth with potencies comparable to homolog **9a**. *para*-Fluorination or chlorination of the R^1 phenyl ring had no impact in the MOLM-13 assay (*p*-fluoro **10c**: GI_{50} = 0.005 μM, and *p*-chloro **10d**: GI_{50} = 0.003 μM), but *p*-fluoro compound **10c** was almost sevenfold less active than the unsubstituted analogue **10a** against FLT3 (**10c**: FLT3 IC_{50} = 0.066 μM). These phenyl-substituted ureas **10a**–**d** had slightly decreased inhibitory potencies against VEGFR2 and aurora A compared to homolog **9a**. Because the SAR of the terminal heteroaryl benzylureas **10** was similar to phenylureas **9**, only representative isoxazol-3-yl compounds **10e**–**g** are shown in Table 1. Compounds **10e**–**g** potently inhibited FLT3 (IC_{50} = 0.004–0.018 μM), VEGFR2 (IC_{50} = 0.018–0.050 μM) and MOLM-13 cells (GI_{50} = 0.002–0.003 μM). However, significant loss of potency against aurora A was observed for these three compounds compared to analogues **9h** and **9m**–**n**, respectively.

According to prior reports, the 3-aminopyrazole moiety is conformationally well suited to form hydrogen bond interactions with the kinase hinge region of the ATP pocket,[25] and 2-methyl-pyrimidine is a known scaffold for kinase inhibitors.[26] Accordingly, we replaced the benzamide group with a 2-methyl-pyrimidine group bearing a solubilizing substituent at the 4-position, giving phenylureas **13** and benzylureas **14a**–**f** (**N**, Fig. 2). As shown in Table 2, pyrimidine **13**, with a phenyl substituent at R^1 and a water-solubilizing *N*-methylpiperazine group at R^2, was less potent against FLT3 (IC_{50} = 0.28 μM), VEGFR2 (IC_{50} = 0.62 μM) and MOLM-13 cells (GI_{50} = 0.16 μM) than the related benzamide **9a** and was, therefore, not optimized further. Nevertheless, benzylurea compounds **14a**–**f** (based upon a 2-methyl-pyrimidine scaffold) were found to have promising potency in vitro. Retaining the *N*-methylpiperazine group, isoxazol-3-yl ureas **14a** and **b** were found to be potent FLT3 inhibitors, with IC_{50} values of 0.021 and 0.035 μM, respectively. Both of them also inhibited growth of MOLM-13 cells with GI_{50} values of <0.01 μM. However, 5-*tert*-butyl-isoxazole **14b** was a more potent inhibitor of VEGFR2, aurora A and MOLM-13 cell growth than 5-methyl-isoxazole **14a**.

Next, we investigated the effects of water-solubilizing substituents on the 4-position of the pyrimidine ring and compared the potencies of compounds **14c**–**e** with *N*-methylpiperazine analogues **14a** and **14b**. *N*-(2-hydroxyethyl)piperazine **14c** had similar potency to *N*-methylpiperazine **14a** in FLT3, VEGFR2, and MOLM-13 cell proliferation assays but was threefold more potent against aurora A. In contrast, 5-*tert*-butyl-isoxazole **14d** bearing a *N*-(2-hydroxyethyl)piperazine group was three- to fourfold weaker in the FLT3, VEGFR2 and aurora A assays, but maintained potency in the cellular assay compared to **14b**. Furthermore, piperazine **14e** was about as potent as **14b** against FLT3 and six- to sevenfold less potent than **14b** in inhibiting VEGFR2 and aurora A. Piperazine **14e** strongly inhibited growth of MOLM-13 cells, with a GI_{50} value of 0.008 μM. Replacing the 5-*tert*-butyl-isoxazole ring of **14e** with 3-chloro substituted benzene ring (**14f**) had no significant effect on potency in any assay. In comparison with FLT3 inhibitor ureas **1**, **2** and **3** currently in clinical development (Table 2), the inhibition of FLT3-mutant MOLM-13 cell growth by some potent urea compounds (**K** and **N**) is comparable to **1** (GI_{50} = 4 nM) and greater than **2** and **3** (GI_{50} = 56 and 37 nM, respectively).

3.2. Kinase inhibition profiles of 9p and 10f

To better understand enzyme inhibition by these potent compounds, **9p** (a phenylurea) and **10f** (a benzylurea) were assayed against a panel of selected protein tyrosine kinases at a concentration of 1.0 μM. As shown in Table 3, both compounds potently inhibited CSF1R (⩾95%), the VEGFR family (VEGFR1, 2 and 3, ⩾86%), FLT3 (100%), PDGFR-α and -β (⩾85%), TRKA (⩾95%), RET (⩾97%) and Tie2 (⩾83%). Regarding other, structurally unrelated tyrosine kinases, phenylurea **9p** moderately inhibited AMPK A1/B1/G1 (70%), aurora B (79%) and SRC (77%), while benzylurea **10f** strongly inhibited AMPK A1/B1/G1 (94%), JAK1 (82%), TYK2 (86%), aurora B and JAK2 (79% in each case).

3.3. Antiproliferative effects of 9p and 10f on leukemia cell lines

We evaluated the effects of **9p** and **10f** on growth of leukemia cells with or without FLT3 mutations (Table 4). In addition to MOLM-13, both compounds inhibited growth of human AML MV4;11 cells harboring FLT3/ITD, with a GI_{50} of 0.002 μM. Compounds **9p** and **10f** were as potent as FLT3 inhibitor **1**, and at least 15-fold more potent than **2** and **3**, in MOLM-13 and MV4;11 cells. In RS4;11 cells (FLT3-wt), the antiproliferative effects of **9p** and **10f** were modest (GI_{50} = 0.4 and 0.9 μM, respectively). Phenylurea **9p** was weakly cytotoxic against K562 human chronic myeloid leukemia cells (expressing wt-BCR/ABL)[13] and U937 human leukemic monocyte lymphoma cells (not expressing FLT3);[27] GI_{50} = 2.3 and 5.5 μM, respectively. In contrast, benzylurea **10f** did not significantly inhibit growth of K562 cells and U937 cells (GI_{50} >10 μM). Both the cell lines, K562 and U937, are not FLT3-dependent cells. The results reveal the specificity of compound **10f** on FLT3 inhibition. Of the urea compounds shown in Table 4, we found that the growth-inhibitory profile of **10f** against various leukemia cell lines was similar to that of urea **1**; **2** appeared to induce lower growth inhibition against RS4;11 (GI_{50} = 9.3 μM).

3.4. Inhibition of FLT3 and STAT5 phosphorylation in cells

Compound **10f** showed promising antiproliferative activity against the human AML cell lines MOLM-13 and MV4;11, with GI_{50} values of 3 and 2 nM, respectively. To examine whether **10f** inhibited phosphorylation of FLT3 and downstream signaling pathways in FLT3-driven cells, MV4;11 cells were cultured with different concentrations of **10f** for 1 h; inhibition of FLT3 and STAT5 phosphorylation was then determined by Western blot analysis (Fig. 3). It was found that compound **10f** suppressed the phosphorylation of FLT3 and STAT5 in MV4;11 cells, with IC_{50} values of 1 nM against p-FLT3 and p-STAT5, respectively.

3.5. Pharmacokinetics, toxicity and in vivo efficacy

5-*tert*-Butyl-isoxazole compounds **9o**, **9p**, **10f** and **10g** were selected for pharmacokinetic evaluation after intravenous (2 mg/kg) or oral (10 mg/kg) administration to rats (Table 5). After iv dosing, each compound demonstrated moderate to long half-life (5.3–17 h), favorable drug exposure ($AUC_{0-inf.}$) (2118–3145 ng/ml), moderate plasma clearance (10.7–13.2 ml/min/kg) and moderate-to-high volume of distribution (3.6–10 l/kg), but oral bioavailability was less than 5%. Due to this poor oral bioavailability in rats, these four compounds were administered intravenously for evaluation of efficacy and acute toxicity in mice. Before proceeding, toxicity was evaluated to allow selection of the least toxic compound and to determine the proper dose range for evaluation of efficacy in the tumor xenograft model. Compounds **9o**, **9p**, **10f** and **10g** were administered intravenously (25 mg/kg) once daily for 5 consecutive days, in normal mice. Compound **10f** was the safest of these compounds. It was well tolerated; no loss of body weight, and no mortality, were observed. Based on its enzyme-inhibitory and antiproliferative potency as well as its favorable pharmacokinetic

Table 3
Kinase inhibition profiles of compounds **9p** and **10f**

Kinase	% Inhibition @ 1 μM[a]	
	9p	**10f**
ABL1	59	21
ABL1 G250E	43	NT[b]
AKT1 (PKB alpha)	−20	−17
AMPK A1/B1/G1	70	94
AURKA (aurora A)	66 (97)[c]	(48)
AURKB (aurora B)	79	79
AURKC (aurora C)	16	NT
BRAF	15	NT
BTK	NT	−6
CDC42 BPA (MRCKA)	−5	−2
CDK2/cyclin A	16	5
CHEK1 (CHK1)	−9 (1)	(2)
CHEK2 (CHK2)	37 (68)	(10)
CSF1R (FMS)	97	95
EPHA1	NT	−20
EPHB2	NT	19
ERBB2 (HER2)	11	−1
FGFR1	NT	48
FLT1 (VEGFR1)	90	99
FLT3	100	100
FLT4 (VEGFR3)	93 (102)	(86)
FRAP1 (mTOR)	−1 (3)	(−1)
GSK3A (GSK3 alpha)	24	6
GSK3B (GSK3 beta)	13	2
IGF1R	33	−1
IKBKB (IKK beta)	NT	−2
IKBKE (IKK epsilon)	12	−5
JAK1	35	82
JAK2	44	79
JAK3	NT	27
KDR (VEGFR2)	97 (88)	(99)
KIT	71	68
MAP2K1 (MEK1)	5	13
MAPK10 (JNK3)	NT	−3
MAPK14 (p38 alpha)	51	3
MAPK8 (JNK1)	2	−3
MET (cMet)	(28)	2 (40)
MST1R (RON)	6	13
NTRK1 (TRKA)	95	98
PDGFRA (PDGFR alpha)	94 (95)	(85)
PDGFRB (PDGFR beta)	87 (99)	(97)
RAF1 (cRAF) Y340D Y341D	6	NT
RET	99	97
RPS6KB1 (p70S6K)	49	41
SRC	77	35
TEK (Tie2)	90	83
TYK2	3	86
TYRO3 (RSE)	NT	24

[a] Percentage inhibition was determined by Invitrogen SelectScreen kinase profiling service.
[b] NT = not tested.
[c] Parenthesis means in-house Kinase-Glo assay.

Table 4
Inhibition of leukemia cell growth by **9p** and **10f**

Cell line	Characterization	GI_{50} (μM)			
		9p	**10f**	**1**	**2**
MOLM-13	AML-FLT3-ITD	0.003	0.003	0.004	0.056
MV4;11	AML-FLT3-ITD	0.002	0.002	0.003	0.043
RS4;11	ALL-wt-FLT3	0.4	0.9	2.2	9.3
K562	CML-Bcr-Abl FLT3-negative	2.3	11.8	>20	7.3
U937	AML-FLT3-negative	5.5	>20	>20	3.4

AML, acute myelocytic leukemia; ALL, acute lymphoblastic leukemia; CML, chronic myelogenous leukemia.

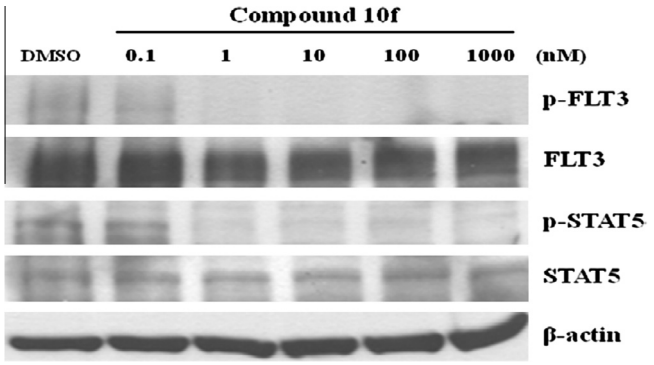

Figure 3. Compound **10f** inhibits FLT3 phosphorylation in MV4;11 AML cells, which are homozygous for FLT-ITD. Cells were treated with **10f** at the indicated concentrations for 1 h. Phosphorylation of FLT3 and STAT5 was evaluated by Western blot analysis.

Table 5
Pharmacokinetic parameters of compounds **9o**, **9p**, **10f** and **10g** in rats[a]

Parameter	Unit	Compound			
		9o	**9p**	**10f**	**10g**
$AUC_{0-inf.}$	ng/ml h	2856	3015	3145	2118
CL	ml/min/kg	13.9	11.3	10.7	17.2
Vd_{ss}	l/kg	4.7	10	3.6	8.0
$t_{1/2}$	h	5.3	17	6.2	11
F	%	4	NT[b]	1	ND[c]

[a] Sprague–Dawley rats were dosed at 2 mg/kg iv ($n = 3$).
[b] NT: not tested.
[c] ND: not detected.

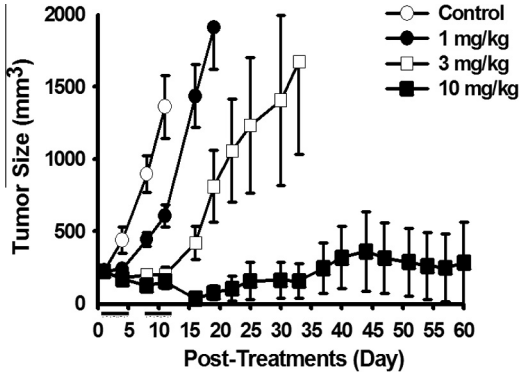

Figure 4. Compound **10f** demonstrates antitumor efficacy after intravenous (iv) administration in the MOLM-13 xenograft model (qd, days 1–5 and 8–12). Tumor size is expressed as the mean ± SEM ($n = 6$–8/group).

profile and low toxicity, compound **10f** was chosen for further in vivo evaluation.

FLT3-ITD-bearing MV4;11 and MOLM-13 xenografts have been widely used to evaluate the in vivo efficacy of FLT3 inhibitors against AML.[7,13] We[19,20] and others[7,28] have found the MV4;11 xenograft model to be noticeably more sensitive to FLT3 inhibitors. To assess the ability of compound **10f** to inhibit tumor growth in an AML xenograft model, efficacy testing of **10f** was therefore conducted using a MOLM-13 tumor xenograft model (Fig. 4). Compound **10f** was administered intravenously (1, 3 and 10 mg/kg qd) on days 1–5 and 8–12; by the end of this period the MOLM-13 tumors reached an average volume of 200 mm^3. At 1 mg/kg, tumor growth was inhibited for the first 5 days, after which tumor growth resumed and tumor growth inhibition (TGI) was observed to be 66% on day 11. At 3 mg/kg, tumor growth was inhibited throughout the dosing period with 7% tumor regression on day 11; tumor growth resumed soon after dosing was halted. At 10 mg/kg, near-complete tumor regression was observed in all animals by day 16 (84% tumor regression); complete regression (CR) occurred in 5 of 7 treated animals during 48 days of post-treatment observation. No loss of body weight was observed in animals treated with any dose of **10f**. In comparison with sulfonamide **4** (1/8 CR, 25 mg/kg)[19] and carbamate **5** (3/7 CR, 25 mg/kg)[21] in the same model, **10f** gave a higher CR ratio (70%) at a lower dose (10 mg/kg). These results demonstrate that **10f** effectively reduces tumor size with 2 weeks of treatment at an intravenous dose of 10 mg/kg/day; **10f** is well tolerated in mice at the effective dose.

4. Conclusion

A rational design approach has been used to identify a novel class of 3-phenyl-1*H*-5-pyrazolylamine-based urea derivatives, which include benzamide (**K**) and pyrimidine (**N**) FLT3 inhibitors. SAR was used to optimize these series, yielding potent FLT3 inhibitors, some of which exhibited comparable antiproliferative potency to the known FLT3 inhibitor **1**, being at least 10-fold more potent than **2** and **3** in MOLM-13 and MV4;11 cells. Broad kinase profiling indicated that phenylurea **9p** and benzylurea **10f** inhibited VEGFR1-3, PDGFRα, PDGFRβ, CSF1R and RET by ⩾85% at 1 μM. In addition, **10f** downregulated the phosphorylation of FLT3/STAT5 in MV4;11 cells, with an IC_{50} of 1 nM, and showed high efficacy and tolerability in the MOLM-13 human AML xenograft model.

5. Experimental

5.1. Chemistry methods

All commercial chemicals and solvents are reagent grade and were used without further treatment unless otherwise noted. ^1H NMR spectra were obtained with a Varian Mercury-300 or a Varian Mercury-400 spectrometer. Chemical shifts were recorded in parts per million (ppm, δ) and were reported relative to the solvent peak or TMS. LC/MS data were measured on an Agilent MSD-1100 ESI-MS/MS System. High-resolution mass spectra (HRMS) were measured with a Thermo Finnigan (TSQ Quantum) electrospray ionization (ESI) mass spectrometer. Flash column chromatography was done using silica gel (Merck Kieselgel 60, No. 9385, 230–400 mesh ASTM). Reactions were monitored by TLC using Merck 60 F_{254} silica gel glass backed plates (5 × 10 cm); zones were detected visually under ultraviolet irradiation (254 nm) or by spraying with phosphomolybdic acid reagent (Aldrich) followed by heating at 80 °C. All starting materials and amines were commercially available unless otherwise indicated. The purity of compounds was determined by a Hitachi 2000 series HPLC system. Except for compounds **9k** and **9n**, purity of target compounds **9** and **10** were over 95% based on reverse phase C_{18} column (Agilent ZORBAX Eclipse XDB-C18 5 μm, 4.6 mm × 150 mm) and reverse phase phenyl column (Waters XBridge Phenly 5 υ m, 4.6 mm × 150 mm) under the following gradient elution condition: Mobile phase A-acetonitrile (10–90%, 0–45 min) and mobile phase B-10 mM NH_4OAc aqueous solution containing 0.1% formic acid (90–10%, 0–45 min). The flow-rate was 0.5 ml/min and the injection volume was 20 μl. The system operated at 25 °C. Peaks were detected at $\lambda = 254$ nm.

5.2. General procedure for the preparation of compounds 9 and 10

The starting materials **6a** and **6b** were synthesized according to the literature report.[22,23] Pyrazolylamine **6** (1.0 equiv) in pyridine

at room temperature was added acyl chloride **7** (1.2 equiv). After 1 h of stirring at room temperature, the reaction mixture was evaporated to dryness and the residue suspended in saturated $NaHCO_3$ solution. The suspension was vigorously stirred at room temperature for 1 h, and the resultant solid was collected by filtration and dried in vacuo. The crude amide was used for the next reaction without further purification. To a solution of crude amide prepared from last step in MeOH was added 6 N HCl (5.0 equiv) and a catalytic amount of 10% Pd/C at room temperature. The mixture was vigorously stirred at room temperature under an atmospheric pressure of hydrogen for 12 h. The catalyst was removed by filtration and the filtrate was concentrated in vacuo. The crude product was purified by flash column chromatography (eluted with CH_2Cl_2/CH_3OH) yielded the desired amine **8**. Only representative compounds **8a** and one of **8b** are selected to show their NMR and mass data.

5.2.1. *N*1-[3-(4-Aminophenyl)-1*H*-5-pyrazolyl]-4-(4-methylpiperazino)benzamide (8aa, R′ = H)

Mp 251–252 °C. ^{1}H NMR (400 MHz, DMSO-d_6): δ 12.41 (s, 1H), 10.43 (s, 1H), 7.91 (d, J = 8.4 Hz, 2H), 7.38 (d, J = 7.6 Hz, 2H), 6.96 (d, J = 8.8 Hz, 2H), 6.71 (s, 1H), 6.59 (d, J = 8.0 Hz, 2H), 5.30 (s, 2H), 3.26 (t, J = 4.2 Hz, 4H), 2.42 (t, J = 4.4 Hz, 4H), 2.21(s, 3H); MS (ES$^+$) m/z calcd for $C_{21}H_{24}N_6O$: 376.20; found: 377.2 (M+H$^+$), 399.2 (M+Na$^+$).

5.2.2. *N*1-[3-(4-Amino-3-methylphenyl)-1*H*-5-pyrazolyl]-4-(4-methylpiperazino)benzamide (8ab, R′ = CH_3)

Mp 272–274 °C. ^{1}H NMR (300 MHz, DMSO-d_6): δ 12.40 (s, 1H), 10.38 (s, 1H), 7.91 (d, J = 8.7 Hz, 2H), 7.31 (s, 1H), 7.27 (d, J = 8.4 Hz, 1H), 6.96 (d, J = 8.7 Hz, 2H), 6.74 (s, 1H), 6.63 (d, J = 8.4 Hz, 1H), 5.06 (s, 2H), 3.26 (br s, 4H), 2.42 (br s, 4H), 2.21 (s, 3H), 2.09 (s, 3H); MS (ES+) m/z calcd for $C_{22}H_{26}N_6O$: 390.21; found: 391.0 (M+H$^+$), 413.0 (M+Na$^+$).

5.2.3. *N*1-[3-(4-Amino-3-chlorophenyl)-1*H*-5-pyrazolyl]-4-(4-methylpiperazino)benzamide (8ac, R′ = Cl)

^{1}H NMR (300 MHz, DMSO-d_6): δ 12.55 (s, 1H), 10.45 (s, 1H), 7.91 (d, J = 9.0 Hz, 2H), 7.60 (d, J = 1.8 Hz, 1H), 7.40 (dd, J = 8.7, 1.8 Hz, 1H), 6.81 (d, J = 8.7 Hz, 2H), 6.83 (d, J = 8.4 Hz, 2H), 5.57 (s, 2H), 3.31–3.29 (m, 4H), 2.51–2.49 (m, 4H), 2.26 (s, 3H); MS (ES$^+$) m/z calcd for $C_{21}H_{23}ClN_6O$: 410.16; found: 411.0 (M+H$^+$).

5.2.4. *N*1–3-[4-(Aminomethyl)phenyl]-1*H*-5-pyrazolyl-4-(4-methylpiperazino)benzamide (8b, R′ = H)

Mp 164–165 °C. ^{1}H NMR (400 MHz, DMSO-d_6): δ 7.89 (d, J = 8.8 Hz, 2H), 7.61 (d, J = 8.4 Hz, 1H), 7.57 (d, J = 8.0 Hz, 1H), 7.12 (d, J = 8.0 Hz, 1H), 7.05 (d, J = 8.4 Hz, 1H), 6.75 (d, J = 8.8 Hz, 2H), 4.01 (s, 1H), 3.61 (s, 1H), 3.10 (br s, 4H), 2.54 (br s, 4H), 2.22 (s, 3H); MS (ES$^+$) m/z calcd for $C_{22}H_{26}N_6O$: 390.22; found: 391.2 (M+H$^+$).

To a solution of **8** (1.0 equiv) in pyridine at room temperature or in DMSO and $NaHCO_3$ (4.0 equiv) at 50 °C was added alkyl or benzyl isocyanate or heteroaryl carbamic acid 4-nitro-phenyl ester (1.2 equiv). After 1 h of stirring at room temperature, the reaction mixture was evaporated to dryness and the residue suspended in saturated $NaHCO_3$ solution. The suspension was vigorously stirred at room temperature for 1 h before the resultant solid was collected by filtration and dried in vacuo. The crude product was purified by flash column chromatography (eluted with CH_2Cl_2/CH_3OH) yielded the desired phenylurea **9** or benzylurea **10**.

5.2.5. *N*1-(3-4-[(Anilinocarbonyl)amino]phenyl-1*H*-5-pyrazolyl)-4-(4-methylpiperazino)benzamide (9a)

Mp 337–338 °C. ^{1}H NMR (400 MHz, DMSO-d_6): δ 12.68 (br s, 1H), 10.54 (s, 1H), 9.22 (s, 1H), 9.11 (s, 1H), 7.93 (d, J = 8.8 Hz, 2H), 7.65 (d, J = 8.8 Hz, 2H), 7.52 (d, J = 8.8 Hz, 2H), 7.45 (d, J = 7.6 Hz, 2H), 7.27 (t, J = 7.6 Hz, 2H), 7.02–6.88 (m, 3H), 6.86 (br s, 1H), 3.40–3.20 (m, 4H, overlapping with water peak), 2.64–2.60 (m, 4H), 2.35 (s, 3H); MS (ES$^+$) m/z calcd for $C_{28}H_{29}N_7O_2$: 495.24; found: 496.2 (M+H$^+$); HRMS (ESI) calcd for $C_{28}H_{30}N_7O_2$: 496.2455; found: 496.2465 (M+H$^+$).

5.2.6. *N*1-[3-(4-[(Ethylamino)carbonyl]aminophenyl)-1*H*-5-pyrazolyl]-4-(4-methylpiperazino)benzamide (9b)

Mp 322–324 °C. ^{1}H NMR (300 MHz, DMSO-d_6): δ 12.67 (s, 1H), 10.47 (s, 1H), 8.57 (s, 1H), 7.93 (d, J = 8.4 Hz, 2H), 7.59 (d, J = 8.4 Hz, 2H), 7.46 (d, J = 8.4 Hz, 2H), 6.97 (d, J = 8.7 Hz, 2H), 6.90 (br s, 1H), 6.17 (t, J = 5.3 Hz, 1H), 3.29–3.26 (m, 4H), 3.16–3.07 (m, 2H), 2.45–2.42 (m, 4H), 2.22 (s, 3H), 1.06 (t, J = 7.2 Hz, 2H); MS(ES$^+$) m/z calcd for $C_{24}H_{29}N_7O_2$: 447.24; found: 448.1 (M+H$^+$); HRMS (ESI) calcd for $C_{24}H_{30}N_7O_2$: 448.2455; found: 448.2465 (M+H$^+$).

5.2.7. *N*1-[3-(4-[(Cyclopropylamino)carbonyl]aminophenyl)-1*H*-5-pyrazolyl]-4-(4-methylpiperazino)benzamide (9c)

Mp 258–259 °C. ^{1}H NMR (400 MHz, DMSO-d_6): δ 12.68 (s, 1H), 10.48 (s, 1H), 8.48 (s, 1H), 7.92 (d, J = 8.8 Hz, 2H), 7.60 (d, J = 8.4 Hz, 2H), 7.47 (d, J = 8.4 Hz, 2H), 6.97 (d, J = 8.8 Hz, 2H), 6.90 (br s, 1H), 6.49 (s, 1H), 3.27 (m, 4H), 4.54 (m, 1H), 2.44 (m, 4H), 2.22 (s, 3H), 0.64 (td, J = 3.4 Hz, 6.0 Hz, 2H), 0.41 (m, 2H); MS (ES$^+$) m/z calcd for $C_{25}H_{29}N_7O_2$: 459.24; found: 460.2 (M+H$^+$); HRMS (ESI) calcd for $C_{25}H_{30}N_7O_2$: 460.2455; found: 460.2465 (M+H$^+$).

5.2.8. *N*1-[3-(4-[(Pyrrolid-1-yl)carbonyl]aminophenyl)-1*H*-5-pyrazolyl]-4-(4-methylpiperazino)benzamide (9d)

Mp 304–305 °C. ^{1}H NMR (400 MHz, DMSO-d_6): δ 12.68 (s, 1H), 10.50 (s, 1H), 8.24 (s, 1H), 7.92 (d, J = 8.4 Hz, 2H), 7.60 (s, 4H), 6.98 (d, J = 8.4 Hz, 2H), 6.90 (s, 1H), 3.38 (t, J = 6.0 Hz, 4H overlapped with water peak), 3.28 (t, J = 6.4 Hz, 4H), 2.46 (t, J = 6.4 Hz, 4H), 2.23 (s, 3H), 1.86 (t, J = 6.0 Hz, 4H); MS (ES$^+$) m/z calcd for $C_{26}H_{31}N_7O_2$: 473.25; found: 474.3 (M+H$^+$); HRMS (ESI) calcd for $C_{26}H_{32}N_7O_2$: 474.2612; found: 474.2622 (M+H$^+$).

5.2.9. *N*1-[3-(4-[(2-Pyridylamino)carbonyl]aminophenyl)-1*H*-5-pyrazolyl]-4-(4-methylpiperazino)benzamide (9e)

Mp 300–302 °C. ^{1}H NMR (300 MHz, DMSO-d_6): δ 10.68 (s, 1H), 10.49 (s, 1H), 9.51 (s, 1H), 8.31 (dd, J = 1.2, 4.8 Hz, 1H), 7.93 (d, J = 8.4 Hz, 2H), 7.82–7.55 (m, 5H), 7.50 (d, J = 8.4 Hz, 2H), 7.10–6.90 (m, 3H), 3.28 (t, J = 4.8 Hz, 4H), 2.44 (t, J = 4.8 Hz, 4H), 2.22 (s, 3H); MS (ES$^+$) m/z calcd for $C_{27}H_{28}N_8O_2$: 496.23; found: 497.0 (M+H$^+$); HRMS (ESI) calcd for $C_{27}H_{29}N_8O_2$: 497.2408; found: 497.2412 (M+H$^+$).

5.2.10. *N*1-[3-(4-[(3-Pyridylamino)carbonyl]aminophenyl)-1*H*-5-pyrazolyl]-4-(4-methylpiperazino)benzamide (9f)

Mp 191–193 °C. ^{1}H NMR (400 MHz, DMSO-d_6): δ 12.75 (s, 1H), 10.53 (s, 1H), 9.53 (s, 2H), 8.62 (d, J = 2.4 Hz, 1H), 8.20 (dd, J = 1.2, 4.8 Hz, 1H), 7.96–7.93 (m, 3H), 7.68 (d, J = 8.8 Hz, 2H), 7.54 (d, J = 8.4 Hz, 2H), 7.32 (dd, J = 8.4, 4.4 Hz, 1H), 6.99 (d, J = 8.8 Hz, 2H), 6.94 (br s, 1H), 3.34 (m, 4H overlapped with water peak), 2.49–2.54 (m, 4H), 2.33 (s, 3H); MS (ES$^+$) m/z calcd for $C_{27}H_{28}N_8O_2$: 496.23; found: 497.0 (M+H$^+$); HRMS (ESI) calcd for $C_{27}H_{29}N_8O_{22}$: 497.2408; found: 497.2417 (M+H$^+$).

5.2.11. *N*1-3-[4-([(5-Methyl-1,3-thiazol-2-yl)amino]carbonylamino)phenyl]-1*H*-5-pyrazolyl-4-(4-methylpiperazino)benzamide (9g)

Mp 275–277 °C. ^{1}H NMR (300 MHz, DMSO-d_6): δ 10.52 (s, 1H), 10.49 (s, 1H), 9.09 (s, 1H), 7.93 (d, J = 9.0 Hz, 2H), 7.89 (d, J = 9.0 Hz, 1H), 7.81 (d, J = 8.7 Hz, 1H), 7.69 (d, J = 8.7 Hz, 2H), 7.60 (d, J = 8.7 Hz, 1H), 7.55 (d, J = 8.7 Hz, 2H),7.04–6.97 (m, 3H), 3.29 (t, J = 4.8 Hz, 4H), 2.45 (t, J = 4.8 Hz, 4H), 2.32 (s, 3H), 2.23 (s, 3H); MS (ES$^+$) m/z calcd for $C_{26}H_{28}N_8O_2S$: 516.21; found: 517.0 (M+H$^+$); HRMS (ESI) calcd for $C_{26}H_{29}N_8O_2S$: 517.2129; found: 517.2136 (M+H$^+$).

5.2.12. *N*1–3-[4-([(5-Methyl-3-isoxazolyl)amino]carbonylamino)phenyl]-1*H*-5-pyrazolyl-4-(4-methylpiperazino)benzamide HCl salt (9h)

Mp 243–245 °C. ^{1}H NMR (400 MHz, DMSO-d_6): δ 10.64 (s, 1H), 10.42 (br s, 1H), 9.61 (s, 1H), 9.23 (s, 1H), 7.97 (d, J = 8.8 Hz, 2H), 7.67 (d, J = 8.8 Hz, 2H), 7.51 (d, J = 8.8 Hz, 2H), 7.06 (d, J = 8.8 Hz, 2H), 6.88 (s, 1H), 6.54 (s, 1H), 4.08–4.00 (m, 2H), 3.54–3.40 (m, 2H, overlapped with water peak), 3.18–3.06 (m, 4H), 2.81 (d, J = 4.4 Hz, 3H), 2.35 (s, 3H); MS (ES$^+$) m/z calcd for $C_{26}H_{28}N_8O_3$: 500.23; found: 501.1 (M+H$^+$); HRMS (ESI) calcd for $C_{26}H_{29}N_8O_3$: 501.2357; found: 501.2368 (M+H$^+$).

5.2.13. *N*1-(3-4-[([5-(*tert*-Butyl)-3-isoxazolyl]aminocarbonyl)amino]phenyl-1*H*-5-pyrazolyl)-4-(4-methylpiperazino)benzamide (9i)

Mp 332–334 °C. ^{1}H NMR (400 MHz, DMSO-d_6): δ 12.74 (s, 1H), 10.51 (s, 1H), 9.58 (s, 1H), 8.99 (s, 1H), 7.92 (d, J = 9.2 Hz, 2H), 7.69 (d, J = 8.4 Hz, 2H), 7.53 (d, J = 8.8 Hz, 2H), 6.99–6.92 (m, 3H), 6.53 (s, 1H), 3.29–3.27 (m, 4H), 2.47–2.43 (m, 4H), 2.23 (s, 3H), 1.27 (s, 9H); MS(ES$^+$) m/z calcd for $C_{29}H_{34}N_8O_3$: 542.28; found: 543.1 (M+H$^+$); HRMS (ESI) calcd for $C_{29}H_{35}N_8O_3$: 543.2827; found: 543.2832 (M+H$^+$).

5.2.14. *N*1-3-[3-Methyl-4-([(5-methyl-3-isoxazolyl)amino]carbonylamino)phenyl]-1*H*-5-pyrazolyl-4-(4-methylpiperazino)benzamide (9j)

Mp 321–323 °C. ^{1}H NMR (400 MHz, DMSO-d_6): δ 12.73 (s, 1H), 10.49 (s, 1H), 9.88 (s, 1H), 8.35 (s, 1H), 7.97–7.91 (m, 3H), 7.60 (s, 1H), 7.55 (d, J = 8.4 Hz, 1H), 6.97 (d, J = 8.0 Hz, 3H), 6.51 (s, 1H), 3.27 (t, J = 4.8 Hz, 4H), 2.42 (t, J = 4.8 Hz, 4H), 2.36 (s, 3H), 2.29 (s, 3H), 2.21 (s, 3H); MS (ES$^+$) m/z calcd for $C_{27}H_{30}N_8O_3$: 514.24; found: 515.2 (M+H$^+$); HRMS (ESI) calcd for $C_{27}H_{31}N_8O_3$: 515.2514; found: 515.2520 (M+H$^+$).

5.2.15. *N*1-3-[3-Chloro-4-([(5-methyl-3-isoxazolyl)amino]carbonylamino)phenyl]-1*H*-5-pyrazolyl-4-(4-methylpiperazino)benzamide (9k)

Mp 240–242 °C. ^{1}H NMR (400 MHz, DMSO-d_6): δ 12.88 (s, 1H), 10.54 (s, 1H), 10.25 (s, 1H), 8.81 (s, 1H), 8.24 (d, J = 8.4 Hz, 1H), 7.94–7.91 (m, 3H), 7.71 (d, J = 8.8 Hz, 1H), 7.05–6.98 (m, 3H), 6.52 (s, 1H), 3.28 (t, J = 4.8 Hz, 4H), 2.44 (t, J = 4.8 Hz, 4H), 2.38 (s, 3H), 2.22 (s, 3H); MS (ES$^+$) m/z calcd for $C_{26}H_{27}ClN_8O_3$: 534.19; found: 535.2 (M+H$^+$); HRMS (ESI) calcd for $C_{26}H_{28}ClN_8O_3$: 535.1967; found: 535.1978 (M+H$^+$). HPLC (C_{18} column): t_R = 19.65 min, 94.0%. HPLC (phenyl column): t_R = 20.26 min, 94.0%.

5.2.16. *N*1-(3-4-[([5-(*tert*-Butyl)-3-isoxazolyl]aminocarbonyl)amino]phenyl-1*H*-5-pyrazolyl)-4-(2-tetrahydro-1*H*-1-pyrrolylethoxy)benzamide (9l)

Mp 256–257 °C. ^{1}H NMR (400 MHz, DMSO-d_6): δ 13.59 (s, 1H), 11.48 (s, 1H), 10.39 (s, 1H), 9.80 (s, 1H), 8.82 (d, J = 8.8 Hz, 2H), 8.50 (d, J = 8.8 Hz, 2H), 8.34 (d, J = 8.4 Hz, 2H), 7.85 (d, J = 8.8 Hz, 2H), 7.77 (br s, 1H), 7.32 (s, 1H), 4.96 (t, J = 5.8 Hz, 2H), 2.11 (s, 9H); MS (ES$^+$) m/z calcd for $C_{30}H_{35}N_7O_4$: 557.64; found: 558.6 (M+H$^+$); HRMS (ESI) calcd for $C_{30}H_{36}N_7O_4$: 558.2823; found: 558.2841 (M+H$^+$).

5.2.17. *N*1-(3-4-[([5-(*tert*-Butyl)-3-isoxazolyl]aminocarbonyl)amino]phenyl-1*H*-5-pyrazolyl)-4-(2-morpholinoethoxy)benzamide (9m)

Mp 270–272 °C. ^{1}H NMR (400 MHz, DMSO-d_6): 12.79 (s, 1H), 10.67 (s, 1H), 9.57 (s, 1H), 8.94 (s, 1H), 8.01 (d, J = 8.8 Hz, 2H), 7.69 (d, J = 8.4 Hz, 2H), 7.53 (d, J = 8.8 Hz, 2H), 7.04 (d, J = 8.8 Hz, 2H), 6.96 (br s, 1H), 6.52 (s, 1H), 4.17 (t, J = 5.8 Hz, 2H), 3.58 (t, J = 4.6 Hz, 4H), 2.71 (t, J = 5.8 Hz, 2H), 2.48–2.47 (m, 4H, overlappimg with solvent peak), 1.30 (s, 9H); MS (ES$^+$) m/z calcd for $C_{30}H_{35}N_7O_5$: 573.27; found: 574.2 (M+H$^+$); HRMS (ESI) calcd for $C_{30}H_{36}N_7O_5$: 574.2772; found: 574.2786 (M+H$^+$).

5.2.18. *N*1-(3-4-[([5-(*tert*-Butyl)-3-isoxazolyl]aminocarbonyl)amino]phenyl-1*H*-5-pyrazolyl)-4-[(4-methylpiperazino)methyl]benzamide (9n)

Mp 247–248 °C. ^{1}H NMR (300 MHz, DMSO-d_6): δ 10.79 (s, 1H), 9.73 (s, 1H), 9.23 (s, 1H), 7.98 (d, J = 8.1 Hz, 2H), 7.69 (d, J = 8.4 Hz, 2H), 7.54 (d, J = 8.4 Hz, 2H), 7.41 (d, J = 8.1 Hz, 2H), 6.97 (s, 1H), 6.52 (s, 1H), 3.51 (d, J = 5.1 Hz, 2H), 3.28 (t, J = 4.8 Hz, 4H), 2.37 (t, J = 4.8 Hz, 4H), 2.16 (s, 3H), 1.30 (s, 9H); MS (ES$^+$) m/z calcd for $C_{30}H_{36}N_8O_3$: 556.29; found: 557.4 (M+H$^+$); HRMS (ESI) calcd for $C_{30}H_{37}N_8O_3$: 557.2983; found: 557.2998 (M+H$^+$). HPLC (C_{18} column): t_R = 22.29 min, 93.3%. HPLC (phenyl column): t_R = 23.54 min, 93.9%.

5.2.19. *N*1-(3-4-[([5-(*tert*-Butyl)-3-isoxazolyl]aminocarbonyl)amino]-3-methylphenyl-1*H*-5-pyrazolyl)-4-(2-morpholinoethoxy)benzamide (9o)

Mp 258–260 °C. ^{1}H NMR (300 MHz, DMSO-d_6): δ 12.77 (s, 1H), 10.69 (s, 1H), 9.98 (s, 1H), 9.41 (s, 1H), 8.38 (s, 1H), 8.01 (t, J = 9.9 Hz, 3H), 7.57 (t, J = 9.9 Hz, 2H), 7.31 (d, J = 5.4 Hz, 2H), 7.05 (s, 1H), 6.48 (s, 1H), 4.16 (t, J = 5.7 Hz, 2H), 3.58 (t, J = 4.5 Hz, 4H), 2.71 (t, J = 5.7 Hz, 2H), 2.50–2.46 (m, 4H, overlapped with DMSO), 2.30 (s 3H), 1.30 (s, 9H); MS (ES$^+$) m/z calcd for $C_{31}H_{37}N_7O_5$:587.28; found: 588.4 (M+H$^+$); HRMS (ESI) calcd for $C_{31}H_{38}N_7O_5$: 588.2934; found: 588.2926 (M+H$^+$).

5.2.20. *N*1-(3-4-[([5-(*tert*-Butyl)-3-isoxazolyl]aminocarbonyl)amino]-3-methylphenyl-1*H*-5-pyrazolyl)-4-[(4-methylpiperazino)methyl]benzamide (9p)

Mp 263–264 °C. ^{1}H NMR (300 MHz, DMSO-d_6): δ 10.78 (s, 1H), 9.95 (s, 1H), 8.35 (s, 1H), 7.99–7.97 (m, 3H), 7.73 (s, 1H), 7.57 (d, J = 8.4 Hz, 1H), 7.41 (d, J = 8.1 Hz, 2H), 7.11 (s, 1H), 6.48 (s, 1H), 3.52 (s, 2H), 3.35 (s, 4H), 2.37 (s, 4H), 2.30 (s, 3H), 2.15 (s, 3H), 1.30 (s, 9H); MS (ES$^+$) m/z calcd for $C_{31}H_{38}N_8O_3$: 570.31; found: 571.4 (M+H$^+$); HRMS (ESI) calcd for $C_{31}H_{39}N_8O_3$: 571.3145; found: 571.3136 (M+H$^+$).

5.2.21. *N*1-[3-(4-[(Anilinocarbonyl)amino]methylphenyl)-1*H*-5-pyrazolyl]-4-(2-morpholinoethoxy)benzamide (10a)

Mp 237–238 °C. ^{1}H NMR (300 MHz, DMSO-d_6): δ 10.71 (s, 1H), 8.56 (s, 1H), 8.01 (d, J = 8.7 Hz, 2H), 7.71 (d, J = 7.8 Hz, 2H), 7.42–7.37 (m, 4H), 7.22 (t, J = 7.8 Hz, 2H), 7.04–7.02 (m, 3H), 6.90 (t, J = 7.2 Hz, 1H), 6.65 (t, J = 5.7 Hz, 1H), 4.32 (d, J = 5.7 Hz, 2H), 4.17 (t, J = 5.7 Hz, 2H), 3.58 (t, J = 4.8 Hz, 4H), 3.38–3.23 (m, 4H), 2.71 (t, J = 5.7 Hz, 2H); MS (ES$^+$) m/z calcd for $C_{30}H_{32}N_6O_4$: 540.25; found: 541.3 (M+H$^+$); HRMS (ESI) calcd for $C_{30}H_{33}N_6O_4$: 541.2558; found: 541.2569 (M+H$^+$).

5.2.22. *N*1-[3-(4-[(Anilinocarbonyl)amino]methylphenyl)-1*H*-5-pyrazolyl]-4-[(4-methylpiperazino)methyl]benzamide (10b)

Mp 235–237 °C. ^{1}H NMR (300 MHz, DMSO-d_6): δ 12.91 (s, 1H), 10.80 (s, 1H), 8.63 (s, 1H), 7.98 (d, J = 8.4 Hz, 2H), 7.72 (d, J = 8.4 Hz, 2H), 7.43–7.37 (m, 6H), 7.23 (t, J = 7.2 Hz, 2H), 7.03 (s, 1H), 6.90 (d, J = 7.2 Hz, 1H), 6.68 (t, J = 6.0 Hz, 1H), 4.33 (d, J = 6.0 Hz, 2H), 3.52 (s, 2H), 2.37 (br s, 8H), 2.16 (s, 3H); MS (ES$^+$) m/z calcd for $C_{30}H_{33}N_7O_2$: 523.27; found: 524.3 (M+H$^+$); HRMS (ESI) calcd for $C_{30}H_{34}N_7O_2$: 524.2768; found: 524.2773 (M+H$^+$).

5.2.23. *N*1-[3-(4-[([4-Fluorophenyl]aminocarbonyl)amino]methylphenyl)-1*H*-5-pyrazolyl]-4-(2-morpholinoethoxy)benzamide (10c)

Mp 238–240 °C. ^{1}H NMR (300 MHz, DMSO-d_6): δ 12.87 (s, 1H), 10.67 (s, 1H), 8.63 (s, 1H), 8.00 (d, J = 8.7 Hz, 2H), 7.71 (d, J = 8.1 Hz, 2H), 7.44–7.35 (m, 4H), 7.10–7.02 (m, 4H), 6.65 (t,

J = 6.0 Hz, 1H), 4.32 (d, *J* = 6.0 Hz, 2H), 4.17 (t, *J* = 5.7 Hz, 2H), 3.58 (t, *J* = 4.8 Hz, 4H), 2.71 (t, *J* = 5.7 Hz, 2H), 2.50–2.46 (m, 4H, overlapping with DMSO peak); MS (ES^+) *m*/*z* calcd for $C_{30}H_{31}FN_6O_4$: 558.24; found: 559.2 ($M+H^+$); HRMS (ESI) calcd for $C_{30}H_{32}FN_6O_4$: 559.2464; found: 559.2468 ($M+H^+$).

5.2.24. *N*1-[3-(4-[([4-Chloro-phenyl]aminocarbonyl)amino]methylphenyl)-1*H*-5-pyrazolyl]-4-(2-morpholinoethoxy)benzamide (10d)

Mp 228–229 °C. ^1H NMR (400 MHz, DMSO-d_6): δ 12.87 (s, 1H), 10.68 (s, 1H), 8.76 (s, 1H), 8.01 (d, *J* = 8.8 Hz, 2H), 7.72 (d, *J* = 8.0 Hz, 2H), 7.45 (d, *J* = 8.4 Hz, 2H), 7.37 (d, *J* = 7.6 Hz, 2H), 7.27 (d, *J* = 8.4 Hz, 2H), 7.04 (d, *J* = 8.0 Hz, 2H), 6.72 (t, *J* = 5.6 Hz, 1H), 4.32 (d, *J* = 6.0 Hz, 2H), 4.17 (t, *J* = 5.6 Hz, 2H), 3.58 (t, *J* = 4.8 Hz, 4H), 2.71 (t, *J* = 5.6 Hz, 2H), 2.50–2.48 (m, 4H, overlapping with DMSO peak); MS (ES^+) *m*/*z* calcd for $C_{30}H_{31}ClN_6O_4$: 574.21; found: 575.2 ($M+H^+$); HRMS (ESI) calcd for $C_{30}H_{32}ClN_6O_4$: 575.2174; found: 575.2186 ($M+H^+$).

5.2.25. *N*1-(3-4-[([(5-Methyl-3-isoxazolyl)amino]carbonylamino)methyl]phenyl-1*H*-5-pyrazolyl)-4-(4-methylpiperazino)benzamide (10e)

Mp 259–260 °C. ^1H NMR (400 MHz, DMSO-d_6): δ 12.83 (s, 1H), 10.52 (s, 1H), 9.42 (s, 1H), 7.91 (d, *J* = 8.0 Hz, 2H), 7.69 (d, *J* = 7.6 Hz, 2H), 7.33 (d, *J* = 7.6 Hz, 2H), 7.03–6.88 (m, 4H), 6.39 (s, 1H), 4.32 (d, *J* = 5.2 Hz, 2H), 3.28–3.18 (m, 4H), 2.48–2.38 (m, 4H), 2.31 (s, 3H), 2.20 (s, 3H); MS (ES^+) *m*/*z* calcd for $C_{27}H_{30}N_8O_3$: 514.24; found: 515.3 ($M+H^+$); HRMS (ESI) calcd for $C_{27}H_{31}N_8O_3$: 515.2514; found: 515.2518 ($M+H^+$).

5.2.26. *N*1-[3-(4-[([5-(*tert*-Butyl)-3-isoxazolyl]aminocarbonyl)amino]methylphenyl)-1*H*-5-pyrazolyl]-4-(2-morpholinoethoxy)benzamide (10f)

Mp 250–252 °C. ^1H NMR (400 MHz, DMSO-d_6): δ 12.87 (s, 1H), 10.68 (s, 1H), 9.48 (s, 1H), 8.00 (d, *J* = 8.0 Hz, 2H), 7.71 (d, *J* = 7.2 Hz, 2H), 7.35 (d, *J* = 7.6 Hz, 2H), 7.03 (d, *J* = 8.0 Hz, 2H), 7.00 (s, 1H), 6.38 (s, 1H), 4.33 (t, *J* = 5.2 Hz, 2H), 4.16 (t, *J* = 5.6 Hz, 2H), 3.57 (t, *J* = 4.4 Hz, 4H), 2.70 (t, *J* = 5.2 Hz, 2H), 2.49–2.47 (m, 4H, overlapped with DMSO), 1.27 (s, 9H); MS (ES^+) *m*/*z* calcd for $C_{31}H_{37}N_7O_5$: 587.28; found: 588.3 ($M+H^+$); HRMS (ESI) calcd for $C_{31}H_{38}N_7O_5$: 588.2929; found: 588.2934 ($M+H^+$).

5.2.27. *N*1-[3-(4-[([5-(*tert*-Butyl)-3-isoxazolyl]aminocarbonyl)amino]methylphenyl)-1*H*-5-pyrazolyl]-4-[(4-methylpiperazino)methyl]benzamide (10g)

Mp 226–227 °C. ^1H NMR (300 MHz, DMSO-d_6): δ 10.82 (s, 1H), 10.71 (s, 1H), 9.50 (s, 1H), 7.98 (d, *J* = 8.1 Hz, 2H), 7.72 (d, *J* = 8.1 Hz, 2H), 7.41 (d, *J* = 8.1 Hz, 2H), 7.36 (t, *J* = 8.4 Hz, 2H), 7.02 (t, *J* = 5.7 Hz, 2H), 6.38 (s, 1H), 4.35 (d, *J* = 5.7 Hz, 2H), 3.52 (s, 2H), 3.25 (s, 4H), 2.37 (s, 4H), 2.15 (s, 3H), 1.27 (s, 9H); MS (ES^+) *m*/*z* calcd for $C_{31}H_{38}N_8O_3$: 570.31; found: 571.4 ($M+H^+$); HRMS (ESI) calcd for $C_{31}H_{39}N_8O_3$: 571.3140; found: 571.3147 ($M+H^+$).

5.3. General procedure for the preparation of compounds 13 and 14

To a solution of **6** (1.0 equiv) and 4,6-dichloro-2-methylpyrimidine (1.5 equiv) in DMF at room temperature was added hydrogen chloride solution (4.0 M in dioxane, 1.6 equiv) and the resultant mixture was stirred at 80 °C for 4 h. After cooling to room temperature, the solvent was evaporated in vacuo to give a viscous residue, which was partitioned between EtOAc and saturated $NaHCO_3$ solution. The organic layer was separated, dried over $MgSO_4$ and concentrated in vacuo. Purification by flash column chromatography (eluted with CH_2Cl_2/CH_3OH) yielded compound **11**. Only **11b** is selected to show its NMR and mass data.

5.3.1. (4-[5-(6-Chloro-2-methyl-pyrimidin-4-ylamino)-1*H*-pyrazol-3-yl]benzyl)carbamic acid benzyl ester (11b)

Mp 208–209 °C. ^1H NMR (400 MHz, DMSO-d_6): δ 12.85 (s, 1H), 10.26 (s, 1H), 7.85 (t, *J* = 6.0 Hz, 1H), 7.67 (d, *J* = 7.8 Hz, 1H), 7.20–7.50 (m, 7H), 6.63 (br s, 1H), 5.04 (s, 2H), 4.22 (d, *J* = 6.0 Hz, 2H), 2.44 (s, 3H); MS (ES^+) *m*/*z* calcd for $C_{23}H_{21}ClN_6O_2$: 448.14 and 450.14; found: 449.1 and 451.1 ($M+H^+$).

To a solution of **11** (1.0 equiv) in pyridine at room temperature was added 1° or 2° amines (2.0 equiv) and the resultant mixture was stirred at 80 °C for 2 h. After cooling to room temperature, the reaction mixture was evaporated to dryness and the residue suspended in saturated $NaHCO_3$ solution. The suspension was vigorously stirred at room temperature for 1 h, and the resultant solid was collected by filtration and dried in vacuo to yield crude product which was used without further purification. To a solution of the crude product prepared from last step in MeOH was added 12 N HCl (5.0 equiv) and a catalytic amount of 10% Pd/C at room temperature. The mixture was vigorously stirred at room temperature under an atmospheric pressure of hydrogen for 12 h. The catalyst was removed by filtration and the filtrate was concentrated in vacuo. The crude amine was used for the next reaction without further purification. Starting with the crude amine, the same procedures were followed as described in the synthesis of ureas **9**–**10** to yield compounds **13**–**14**.

5.3.2. *N*-[4-(5-[2-Methyl-6-(4-methylpiperazino)-4-pyrimidinyl]amino-1*H*-3-pyrazolyl)phenyl]-*N*′-phenylurea (13)

^1H NMR (400 MHz, DMSO-d_6): δ 12.58 (s, 1H), 9.32 (s, 1H), 8.88 (s, 1H), 8.78 (s, 1H), 7.61 (d, *J* = 8.8 Hz, 2H), 7.57 (d, *J* = 4.4 Hz, 1H), 7.52 (d, *J* = 8.8 Hz, 2H), 7.45–7.27 (m, 3H), 6.96 (t, *J* = 7.2 Hz, 1H), 6.63 (s, 1H), 6.38 (s, 1H), 3.41 (br s, 6H), 2.37 (br s, 3H), 2.28 (s, 3H), 2.20 (s, 2H); MS (ES^+) *m*/*z* calcd for $C_{26}H_{29}N_9O$: 483.25; found: 484.1 ($M+H^+$).

5.3.3. *N*-(5-Methyl-3-isoxazolyl)-*N*′-4-(5-[2-methyl-6-(4-methylpiperazino)-4-pyrimidinylamino]-1*H*-3-pyrazolyl)benzylurea (14a)

Mp 154–156 °C. ^1H NMR (400 MHz, DMSO-d_6): δ 12.67 (s, 1H), 9.40 (s, 1H), 9.34 (s, 1H), 7.66 (d, *J* = 8.4 Hz, 2H), 7.34 (d, *J* = 8.4 Hz, 2H), 7.03 (t, *J* = 6.0 Hz, 1H), 6.63 (br s, 1H), 6.54 (s, 1H), 6.44 (s, 1H), 4.34 (d, *J* = 5.6 Hz, 2H), 3.48 (m, 4H), 2.36 (t, *J* = 4.8 Hz, 4H), 2.33 (s, 3H), 2.29 (s, 3H), 2.21 (s, 3H); MS (ES^+) *m*/*z* calcd for $C_{258}H_{30}N_{10}O_2$: 502.58; found: 503.1 ($M+H^+$).

5.3.4. *N*-[5-(*tert*-Butyl)-3-isoxazolyl]-*N*′-4-(5-[2-methyl-6-(4-methylpiperazino)-4-pyrimidinylamino]-1*H*-3-pyrazolyl)benzylurea (14b)

Mp 166–167 °C. ^1H NMR (400 MHz, DMSO-d_6): δ 12.70 (s, 1H), 9.49 (s, 1H), 9.31 (s, 1H), 7.66 (d, *J* = 7.2 Hz, 2H), 7.34 (d, *J* = 8.0 Hz, 2H), 7.01 (t, *J* = 6.0 Hz, 1H), 6.69 (s, 1H), 6.46 (s, 1H), 6.37 (m, 1H), 4.33 (d, *J* = 6.0 Hz, 2H), 3.48 (d, *J* = 4.8 Hz, 4H), 2.36 (t, *J* = 4.8 Hz, 4H), 2.28 (s, 3H), 2.20 (s, 3H), 1.26 (s, 9H); MS (ES^+) *m*/*z* calcd for $C_{28}H_{36}N_{10}O_2$: 544.30; found: 545.3 ($M+H^+$); HRMS (ESI) calcd for $C_{28}H_{37}N_{10}O_2$: 545.3101; found: 545.3098 ($M+H^+$).

5.3.5. *N*-(5-Methyl-3-isoxazolyl)-*N*′-4-[5-(6-[4-(2-hydroxyethyl)piperazino]-2-methyl-4-pyrimidinylamino)-1*H*-3-pyrazolyl]benzylurea (14c)

Mp 105–107 °C. ^1H NMR (400 MHz, DMSO-d_6): δ 12.69 (s, 1H), 9.43 (s, 1H), 9.31 (s, 1H), 7.66 (d, *J* = 7.2 Hz, 2H), 7.33 (d, *J* = 7.6 Hz, 2H), 7.03 (t, *J* = 5.6 Hz, 1H), 6.65 (s, 1H), 6.40–6.60 (m, 1H), 6.39 (s, 1H), 4.46 (s, 1H), 4.33 (d, *J* = 5.6 Hz, 2H), 3.38–3.60 (m, 8H), 2.40–2.55 (m, 4H overlapped with DMSO peak), 2.36 (s, 3H), 2.28 (s, 3H); MS (ES^+) *m*/*z* calcd for $C_{26}H_{32}N_{10}O_3$: 532.60; found: 533.3 ($M+H^+$); HRMS (ESI) calcd for $C_{26}H_{33}N_{10}O_3$: 533.2737; found: 533.2736 ($M+H^+$).

5.3.6. *N*-[5-(*tert*-Butyl)-3-isoxazolyl]-*N′*-4-[5-(6-[4-(2-hydroxyethyl)piperazino]-2-methyl-4-pyrimidinylamino)-1*H*-3-pyrazolyl]benzylurea (14d)

Mp 155–157 °C. ^{1}H NMR (300 MHz, DMSO-d_6): δ 12.65 (s, 1H), 9.48 (s, 1H), 9.31 (s, 1H), 7.64 (d, J = 8.1 Hz, 2H), 7.32 (d, J = 8.1 Hz, 2H), 7.00 (t, J = 5.7 Hz, 1H), 6.65 (s, 1H), 6.42 (br s, 1H), 6.35 (s, 1H), 4.43 (t, J = 5.4 Hz,1H), 4.31 (d, J = 5.7 Hz, 2H), 3.40–3.60 (m, 8H), 2.30–2.55 (m, 4H overlapped with DMSO peak), 2.27 (s, 3H), 1.25 (s, 9H); MS (ES$^+$) m/z calcd for $C_{29}H_{38}N_{10}O3$: 574.69; found: 575.3 (M+H$^+$).

5.3.7. *N*-[5-(*tert*-Butyl)-3-isoxazolyl]-*N′*-4-[5-(2-methyl-6-piperazino-4-pyrimidinylamino)-1*H*-3-pyrazolyl]benzylurea (14e)

Mp 74–75 °C. ^{1}H NMR (400 MHz, DMSO-d_6): δ 12.69 (s, 1H), 9.52 (s, 1H), 9.33 (s, 1H), 7.65 (d, J = 7.6 Hz, 2H), 7.33 (d, J = 8.4 Hz, 2H), 7.08 (t, J = 6.0 Hz, 1H), 6.50 (s, 1H), 6.46 (d, J = 6.4 Hz, 1H), 6.36 (m, 1H), 4.32 (d, J = 5.6 Hz, 2H), 3.53–3.49 (m, 4H, overlapped with water peak), 2.91 (t, J = 4.8 Hz, 4H), 2.28 (s, 3H), 1.25 (s, 9H); MS (ES$^+$) m/z calcd for $C_{27}H_{34}N_{10}O_2$: 530.29; found: 531.3 (M+H$^+$); HRMS (ESI) calcd for $C_{27}H_{35}N_{10}O_2$: 531.2944; found: 531.2943 (M+H$^+$).

5.3.8. *N*-(3-Chlorophenyl)-*N′*-4-[5-(2-methyl-6-piperazino-4-pyrimidinylamino)-1*H*-3-pyrazolyl]benzylurea (14f)

Mp 96–97 °C. ^{1}H NMR (400 MHz, DMSO-d_6): δ 10.00 (s, 1H), 9.04 (s, 3H), 7.65–7.75 (m, 3H), 7.36 (d, J = 8.0 Hz, 2H), 7.19–7.23 (m, 2H), 6.99 (t, J = 6.4 Hz, 1H), 6.85–6.88 (m, 1H), 6.57 (s, 1H), 6.50 (s, 1H), 4.30 (d, J = 5.6 Hz, 2H), 3.65–3.83 (m, 4H), 3.12–3.33 (m, 4H), 2.37 (s, 3H); MS (ES$^+$) m/z calcd for $C_{26}H_{28}ClN_9O$: 517.21; found: 518.2 (M+H$^+$); HRMS (ESI) calcd for $C_{26}H_{29}ClN_9O$: 518.2184; found: 518.2182 (M+H$^+$).

5.4. Kinase assays

FLT3: GST-FLT3-KD^{WT} containing the FLT3 kinase catalytic domain (residues Y567∼S993) were expressed in Sf9 insect cells transfected the baculovirus containing pBac-PAK8-GST-FLT3-KD plasmid. The FLT3^{WT} Kinase-Glo assays were carried out in 96-well plates at 30 °C for 4 h and tested compound in a final volume of 50 μl including the following components: 75 ng GST-FLT3-KD^{WT} proteins, 25 mM HEPES, pH 7.4, 4 mM $MnCl_2$, 10 mM $MgCl_2$, 2 mM DTT, 0.02% Triton X-100, 0.1 mg/ml bovine serum albumin, 25 μM Her2 peptide substrate, 0.5 mM Na_3VO_4, and 1 μM ATP. *VEGFR2:* The recombinant GST-VEGFR2 (residues V789-V1356) containing kinase domain were expressed in Sf9 insect cells. The kinase assay were carried out in 96-well plates with tested compound in a final volume of 50 μl reaction at 30 °C for 120 min with following components: 25 mM HEPES pH 7.4, 10 mM $MgCl_2$, 4 mM $MnCl_2$, 0.5 mM Na_3VO_4, 2 mM DTT, 0.02% Triton X100, 0.01% BSA, 1 μM ATP, 2 μM polyGlu4:Tyr peptide, 50∼100 ng recombinant VEGFR2. *Aurora Kinase A*: The recombinant GST-Aurora A (residues S123-S401) containing kinase domain were expressed in Sf9 insect cells. The kinase assay were carried out in 96-well plates with tested compound in a final volume of 50 μl reaction at 37 °C for 90 min with following components: 50 mM Tris–HCl pH 7.4, 10 mM NaCl, 10 mM $MgCl_2$, 0.01% BSA, 5 μM ATP, 1 mM DTT and 15 μM tetra(-LRRASLG) peptide, and 150 ng recombinant Aurora A.

Following incubation, 50 μl Kinase-Glo Plus Reagent (Promega, Madison, WI, USA) was added and the mixture was incubated at 25 °C for 20 min. A 70-μl aliquot of each reaction mixture was transferred to a black microtiter plate and the luminescence was measured on Wallac Vector 1420 multilabel counter (PerkinElmer, Shelton, CT, USA).

5.5. Western blot analysis

Cultured cells were suspended in lysis buffer (50 mM Tris, pH 8.0, 150 mM NaCl, 1% Triton X-100, 0.5% sodium deoxycholate, 0.1% SDS, 1 mM sodium orthovanadate, 1 mM PMSF, and 1 mM DTT). Cell lysates were kept on ice for 10 min and then cleared by centrifugation at 14,000×g for 15 min at 4 °C. After adding 5× sample buffer, the supernatants were heated at 95 °C for 5 min, and cell extract samples (10 or 20 μg) were separated by 10% or 15% SDS–PAGE and transferred onto a polyvinylidene difluoride membrane (Millipore, Bedford, MA, USA). The membrane was then probed using the indicated primary antibodies anti-β-*actin* (Santa Cruz Biotechnology, Santa Cruz, CA, USA), and the following antibodies including anti-*Stat5*, anti-*phospho-Stat5* (Tyr^{694}), anti-FLT3, anti-phospho-FLT3 (Tyr^{591}) from Cell Signaling Technology (Danvers, MA, USA). After the membrane was first incubated with primary antibody in TBST buffer (20 mM Tris pH 7.5, 135 mM NaCl, and 0.1% (v/v) Tween 20) with 5% (wt/v) milk powder (or 2% (wt/v) bovine serum albumin) and washed with TBST buffer, the membrane then blotted with horseradish peroxidase–conjugated secondary antibody (1:1000 dilution). The membrane was then developed with SuperSignal reagent (Pierce, Rockford, IL, USA) upon exposure to X-ray film.

5.6. Cell lines and MTS cell viability assays

The leukemias cell lines MOLM-13, MV4:11, RSV4;11, U937, and K562 were purchased from American Type Culture Collection (ATCC, Manassas, VA, USA). All leukemias cell lines were maintained in RPMI 1640 medium supplemented with 10% fetal bovine serum (FBS), 10 U/ml penicillin, and 10 g/ml streptomycin at 37 °C and 5% CO_2. To determine cell viability after drug treatment, assays were performed by seeding 10,000 cells (leukemias cell lines) per well in a 96-well culture plate. After 16 h, cells were then treated with vehicle or various concentrations of compound in medium for 72 h. Viable cells were quantitated using the MTS method (Promega, Madison, WI, USA) according to the manufacturer's recommended protocol. The results were determined by measuring the absorbance at 490 nm using a plate reader (Victor2; PerkinElmer, Shelton, CT, USA). The IC_{50} value was defined as the amount of compound that caused 50% reduction in cell viability in comparison with DMSO-treated (vehicle) control and was calculated using Prism version 4 software (GraphPad, San Diego, CA, USA).

5.7. Pharmacokinetics

Male Sprague–Dawley rats weighing 300–400 g each (8–12 weeks old) were obtained from BioLASCO (Taiwan Co., Ltd, Ilan, Taiwan). The animal studies were performed according to NHRI institutional animal care and committee-approved procedures. Animals were surgically prepared with a jugular-vein cannula 1 day before dosing and fasted overnight (for approximately 18–20 h) before dosing. Water was available ad libitum throughout the experiment. Food was provided at 4 h after dosing. A single 2.0 mg/kg and 10 mg/kg dose of compound, as a PEG400/DMA (80/20, v/v) solution, was separately administered to groups of 3 rats each intravenously (iv) and oral gavage, respectively. Each animal received 2 or 10 ml of the dosing solution per kg of body weight for iv and po, respectively. At 0 (before dosing), 2, 5 (iv only), 15, and 30 min and at 1, 2, 4, 6, 8, and 24 h after dosing, a blood sample (0.15 ml) was collected from each animal through the jugular-vein cannula and stored in ice (0–4 °C). Immediately after collecting the blood sample, 150 ml of physiological saline (containing 30 Units of heparin per ml) was injected into the rat through the jugular-vein cannula. Plasma was separated from the

blood by centrifugation (14,000 g for 15 min at 4 °C in a Beckman Model AllegraTM 6R centrifuge) and stored in a freezer (−20 °C). All samples were analyzed for the parent drug by LC–MS/MS. Data were acquired through selected reaction ion monitoring. Plasma concentration data were analyzed with non-compartmental method.

5.8. Efficacy in tumor xenograft model

Nine weeks old athymic nu/nu nude mice were obtained from BioLASCO, Taiwan Co., Ltd (Ilan, Taiwan). The mice were housed in sterilized cages equipped with an air filter and sterile bedding materials at the Laboratory Animal Center. All mice were fed with sterilized water and chow under 12-h light/dark schedule. 100 μl suspensions of MOLM-13 cells (final concentration: 1×10^7 cells/ml; 1×10^6/flank) were transplanted sc into the left flank of nu/nu nude mice. Tumor diameters are measured with digital calipers, and the tumor volume in mm^3 is calculated by the formula: Volume = (length × width^2)/2. In Figure 4, tumor-bearing mice were randomized when the mean tumor volume was ~200 mm^3. The mice were randomly divided into 3 groups of 6–8 animals each, and the treatment was initiated. Compound **10f** was dissolved in vehicle formulation (10% DMSO/20% Cremophor EL/70% saline, v/v/v) and intravenously administrated at 1, 3 and 10 mg/kg once a day for two continuous weeks (on days 1–5 and 8–12). A vehicle control group received intravenously in the same manner. (Animal Use Protocol for this project has been approved by National Health Research Institutes, the protocol No: NHRI-IACUC-100023-A.)

Acknowledgments

The National Health Research Institutes and National Science Council of Taiwan (NSC 100-2325-B-400-002-) financially supported the study.

References and notes

1. Stirewalt, D. L.; Radich, J. P. *Nat. Rev. Cancer* **2003**, *3*, 650.
2. Gilliland, D. G.; Griffin, J. D. *Blood* **2002**, *100*, 1532.
3. Ji, Z.; Ahmed, A. A.; Albert, D. H.; Bouska, J. J.; Bousquet, P. F.; Cunha, G. A.; Diaz, G.; Glaser, K. B.; Guo, J.; Harris, C. M.; Li, J.; Marcotte, P. A.; Moskey, M. D.; Oie, T.; Pease, L.; Soni, N. B.; Stewart, K. D.; Davidsen, S. K.; Michaelides, M. R. *J. Med. Chem.* **2008**, *51*, 1231.
4. Gschwind, A.; Fisher, O. M.; Ullrich, A. *Nat. Rev. Cancer* **2004**, *4*, 361.
5. Vieth, M.; Sutherland, J. J.; Robertson, D. H.; Campbell, R. M. *Drug Discovery Today* **2005**, *10*, 839.
6. Tallman, M.; Gilliland, D.; Rowe, J. *Blood* **2005**, *106*, 1154.
7. Shankar, D. B.; Li, J.; Tapang, P.; Owen McCall, J.; Pease, L. J.; Dai, Y.; Wei, R. Q.; Albert, D. H.; Bouska, J. J.; Osterling, D. J.; Guo, J.; Marcotte, P. A.; Johnson, E. F.; Soni, N.; Hartandi, K.; Michaelides, M. R.; Davidsen, S. K.; Priceman, S. J.; Chang, J. C.; Rhodes, K.; Shah, N.; Moore, T. B.; Sakamoto, K. M.; Glaser, K. B. *Blood* **2007**, *109*, 3400.
8. Levis, M.; Small, D. *Int. J. Hematol.* **2005**, *82*, 100.
9. Kikushige, Y.; Yoshimoto, G.; Miyamoto, T.; Iino, T.; Mori, Y.; Iwasaki, H.; Niiro, H.; Takenaka, K.; Nagafuji, K.; Harada, M.; Ishikawa, F.; Akashi, K. *J. Immunol.* **2008**, *180*, 7358.
10. Mizuki, M.; Fenski, R.; Halfter, H.; Matsumura, I.; Schmidt, R.; Müller, C.; Grüning, W.; Kratz-Albers, K.; Serve, S.; Steur, C.; Büchner, T.; Kienast, J.; Kanakura, Y.; Berdel, W. E.; Serve, H. *Blood* **2000**, *96*, 3907.
11. Abu-Duhier, F. M.; Goodeve, A. C.; Wilson, G. A.; Care, R. S.; Peake, I. R.; Reilly, J. T. *Br. J. Haematol.* **2001**, *113*, 983.
12. Ozeki, K.; Kiyoi, H.; Hirose, Y.; Iwai, M.; Ninomiya, M.; Kodera, Y.; Miyawaki, S.; Kuriyama, K.; Shimazaki, C.; Akiyama, H.; Nishimura, M.; Motoji, T.; Shinagawa, K.; Takeshita, A.; Ueda, R.; Ohno, R.; Emi, N.; Naoe, T. *Blood* **1901**, *2004*, 103.
13. Shiotsu, Y.; Kiyoi, H.; Ishikawa, Y.; Tanizaki, R.; Shimizu, M.; Umehara, H.; Ishii, K.; Mori, Y.; Ozeki, K.; Minami, Y.; Abe, A.; Maeda, H.; Akiyama, T.; Kanda, Y.; Sato, Y.; Akinaga, S.; Naoe, T. *Blood* **2009**, *114*, 1607.
14. Chao, Q.; Sprankle, K. G.; Grotzfeld, R. M.; Lai, A. G.; Carter, T. A.; Velasco, A. M.; Gunawardane, R. N.; Cramer, M. D.; Gardner, M. F.; James, J.; Zarrinkar, P. P.; Patel, H. K.; Bhagwat, S. S. *J. Med. Chem.* **2009**, *52*, 7808.
15. Auclair, D.; Miller, D.; Yatsula, V.; Pickett, W.; Carter, C.; Chang, Y.; Zhang, X.; Wilkie, D.; Burd, A.; Shi, H.; Rocks, S.; Gedrich, R.; Abriola, L.; Vasavada, H.; Lynch, M.; Dumas, J.; Trail, P. A.; Wilhelm, S. M. *Leukemia* **2007**, *21*, 439.
16. Dai, Y.; Hartandi, K.; Ji, Z.; Ahmed, A. A.; Albert, D. H.; Bauch, J. L.; Bouska, J. J.; Bousquet, P. F.; Cunha, G. A.; Glaser, K. B.; Harris, C. M.; Hickman, D.; Guo, J.; Li, J.; Marcotte, P. A.; Marsh, K. C.; Moskey, M. D.; Martin, R. L.; Olson, A. M.; Osterling, D. J.; Pease, L. J.; Soni, N. B.; Stewart, K. D.; Stoll, V. S.; Tapang, P.; Reuter, D. R.; Davidsen, S. K.; Michaelides, M. R. *J. Med. Chem.* **2007**, *50*, 1584.
17. Ustun, C.; DeRemer, D. L.; Jillella, A. P.; Bhalla, K. N. *Expert Opin. Investig. Drugs* **2009**, *18*, 1445.
18. Zarrinkar, P. P.; Gunawardane, R. N.; Cramer, M. D.; Gardner, M. F.; Brigham, D.; Belli, B.; Karaman, M. W.; Pratz, K. W.; Pallares, G.; Chao, Q.; Sprankle, K. G.; Patel, H. K.; Levis, M.; Armstrong, R. C.; James, J.; Bhagwat, S. S. *Blood* **2009**, *114*, 2984.
19. Lin, W. H.; Jiaang, W. T.; Chen, C. W.; Yen, K. J.; Hsieh, S. Y.; Yen, S. C.; Chen, C. P.; Chang, K. Y.; Chang, C. Y.; Chang, T. Y.; Huang, Y. L.; Yeh, T. K.; Chao, Y. S.; Chen, C. T.; Hsu, J. T.-A. *Br. J. Cancer* **2012**, *106*, 475.
20. Lin, W. H.; Hsieh, S. Y.; Yen, S. C.; Chen, C. T.; Yeh, T. K.; Hsu, T.; Lu, C. T.; Chen, C. P.; Chen, C. W.; Chou, L. H.; Huang, Y. L.; Cheng, A. H.; Chang, Y. I.; Tseng, Y. J.; Yen, K. R.; Chao, Y. S.; Hsu, J. T.-A.; Jiaang, W. T. *Bioorg. Med. Chem.* **2011**, *19*, 4173.
21. Hsu, J. T.-A.; Yeh, T. K.; Yen, S. C.; Chen, C. T.; Hsieh, S. Y.; Hsu, T.; Lu, C. T.; Chen, C. H.; Chou, L. H.; Chiu, C. H.; Chang, Y. I.; Tseng, Y. J.; Yen, K. R.; Chao, Y. S.; Lin, W. H.; Jiaang, W. T. *Bioorg. Med. Chem. Lett.* **2012**, *22*, 4654.
22. Moe, S. T.; Thompson, A. B.; Smith, G. M.; Fredenburg, R. A.; Stein, R. L.; Jacobson, A. R. *Bioorg. Med. Chem.* **2009**, *17*, 3072.
23. Nenaidenko, V. G.; Golubinskii, I. V.; Lenkova, O. N.; Shastin, A. V.; Balenkova, E. S. *Russ. J. Org. Chem.* **2004**, *40*, 1518.
24. Grese, T. A.; Cho, S.; Finley, D.; Godfrey, A. G.; Jones, C. D.; Lugar, C. W.; Martin, M. J.; Matsumoto, K.; Pennington, L. D.; Winter, M. W.; Adrian, M. D.; Cole, H. W.; Magee, D. E.; Phillips, D. L.; Rowley, E. R.; Short, L. L.; Glasebrook, A. L.; Bryant, H. U. *J. Med. Chem.* **1997**, *40*, 146.
25. Fancelli, D.; Berta, D.; Bindi, S.; Cameron, A.; Cappella, P.; Carpinelli, P.; Catana, C.; Forte, B.; Giordano, P.; Giorgini, M. L.; Mantegani, S.; Marsiglio, A.; Meroni, M.; Moll, J.; Pittalà, V.; Roletto, F.; Severino, D.; Soncini, C.; Storici, P.; Tonani, R.; Varasi, M.; Vulpetti, A.; Vianello, P. *J. Med. Chem.* **2005**, *48*, 3080.
26. Lombardo, L. J.; Lee, F. Y.; Chen, P.; Norris, D.; Barrish, J. C.; Behnia, K.; Castaneda, S.; Cornelius, L. A.; Das, J.; Doweyko, A. M.; Fairchild, C.; Hunt, J. T.; Inigo, I.; Johnston, K.; Kamath, A.; Kan, D.; Klei, H.; Marathe, P.; Pang, S.; Peterson, R.; Pitt, S.; Schieven, G. L.; Schmidt, R. J.; Tokarski, J.; Wen, M. L.; Wityak, J.; Borzilleri, R. M. *J. Med. Chem.* **2004**, *47*, 6658.
27. Yao, Q.; Nishiuchi, R.; Li, Q.; Kumar, A. R.; Hudson, W. A.; Kersey, J. H. *Clin. Cancer Res.* **2003**, *9*, 4483.
28. Hart, S.; Goh, K. C.; Novotny-Diermayr, V.; Tan, Y. C.; Madan, B.; Amalini, C.; Ong, L. C.; Kheng, B.; Cheong, A.; Zhou, J.; Chng, W. J.; Wood, J. M. *Blood Cancer J.* **2011**, *1*, e44.